TC.
YEDITEPE UNIVERSITY
INSTITUTE OF HEALTH SCIENCES
DEPARTMENT OF HISTOLOGY AND EMBRYOLOGY

DETECTION OF c-ABL TYROSINE KINASE AND THE MAMMALIAN TARGET OF RAPAMYCIN (mTOR) REGULATION IN MOUSE OOCYTE MATURATION

MASTER OF HISTOLOGY AND EMBRYOLOGY THESIS

MELEK OBAIDEEN

İstanbul-2022

TC.
YEDITEPE UNIVERSITY
INSTITUTE OF HEALTH SCIENCES
DEPARTMENT OF HISTOLOGY AND EMBRYOLOGY

DETECTION OF c-ABL TYROSINE KINASE AND THE MAMMALIAN TARGET OF RAPAMYCIN (mTOR) REGULATION IN MOUSE OOCYTE MATURATION

MASTER OF HISTOLOGY AND EMBRYOLOGY THESIS

MELEK OBAIDEEN

SUPERVISOR
Assoc. Prof. Aylin YABA UÇAR

İstanbul-2022

THESIS APPROVAL FORM

Institute : Yeditepe University Institute of Health Sciences

Programme : Master of Histology and Emrbryology

Title of the Thesis : Detection of c-Abl Tyrosine Kinase and The Mammalian Target of Rapamycin (mTOR) Regulation in Mouse Oocyte Maturation

Owner of the Thesis : Melek Obaideen

Examination Date : 24.06.2022

This study have approved as a Master Thesis in regard to content and quality by the Jury.

	Title, Name-Surname (Institution)
Chair of the Jury:	Assoc. Prof. Aylin YABA UÇAR Yeditepe University
Supervisor:	Assoc. Prof. Aylin YABA UÇAR Yeditepe University
Member/Examiner:	Assoc. Prof. Yasemin SEVAL ÇELİK İzmir Ekonomi University
Member/Examiner:	Assist. Prof. Alev CUMBUL Yeditepe University

APPROVAL

This thesis has been deemed by the jury in accordance with the relevant articles of Yeditepe University Graduate Education and Examinations Regulation and has been approved by Administrative Board of Institute with decision dated ..... and numbered .....

Signature
Prof. Bayram YILMAZ
Director of Institute of Health Sciences

DECLARATION

I hereby declare that this thesis is my own work and that, to the best of my knowledge and belief, it contains no material previously published or written by another person nor material which has been accepted for the award of any other degree except where due acknowledgment has been made in the text.

30.06.2022
Melek OBAIDEEN

ACKNOWLEDGEMENTS

In the name of God, and may prayers and peace be upon our prophet Mohammed, Praise be to God whom I can't count his blessings, who facilitated my path to knowledge, and enabled me to complete this university research with his grace, generosity and benevolence. O Lord, all praise is due to you as befits the majesty of your countenance and the greatness of your authority.

After that, I extend my great thanks, great gratitude and deep appreciation to my virtuous teacher and supervisor of my research, to the symbol of sacrifice, giving and patience, to the owner of excellence and bright ideas, she was a beacon in my path to knowledge, to the leader and role model, head of the Department of Histology and Embryology, Assoc. Prof. Aylin Yaba Uçar with all my love and respect.

I also extend my heartfelt thanks and great gratitude to the assistant Ecem Yıldırım, who has supported me in the laboratory.

Thanks a lot, to the honourable members of the discussion committee. With all my love and appreciation to my family, and friends for supporting me throughout my studies.

TABLE OF CONTENTS

LIST OF TABLES

LIST OF FIGURES

LIST OF SYMBOLS/ABBREVIATIONS

AC	Adenylate cyclase
AKT	Protein kinase B
AMPK	5'AMP-activated protein kinase
ATM	Ataxia–telangiectasia mutated
c-ABL	Abelson Tyrosine Kinase
CAMKII	Ca^{2+}/calmodulin-dependent protein kinase II
cAMP	Cyclic adenosine monophosphate
cAMP-PDE	Cyclic adenosine monophosphate- Phosphodiesterase
cCMP	Cyclic guanosine monophosphate
CCs	Cumulus cells
Cdc25B	M-phase inducer phosphatase 2
c-Mos	Proto-oncogene serine/threonine-protein kinase
CP	Cytoplasmic polyadenylation
CPEB	Cytoplasmic polyadenylation element binding protein
CPSF	Cleavage and polyadenylation specificity factor
CSF	Cytostatic factor
DNA-PK	DNA-dependent protein kinase
DSBs	DNA double-strand breaks
4E-BP1	Eukaryotic translation initiation factor 4E-binding protein 1
ElF4E	Eukaryotic translation initiation factor4
eIF4G	Eukaryotic translation initiation factor 4 G
ERK1/2	Extracellular signal-regulated kinases
FKBp12	FK506-binding protein 12
FSH	Follicle-stimulating hormone
GH	Growth hormone
GPR3	G Protein-Coupled Receptor 3
GTP	Guanosine-5'-triphosphate
GV	Germinal vesicle
GVBD	Germinal vesicle breakdown
hCG	Human chorionic gonadotropin
IGF	Insulin-like growth factor
IP3	Inositol trisphosphate

JNK	C-Jun N-terminal kinases
LH	Luteinizing hormone
MAPK	Mitogen-activated protein kinase
MDM2	Mouse double minute 2 homolog
MEK	Dual specificity mitogen-activated protein kinase kinase 1
MGs	Mural granulosa cells
MI	Metaphase I
MII	Metaphase II
MPF	Maturation promotor factor
mRNA	Messenger ribonucleic acid
MS	Meiotic spindle
mtDNA	Mitochondrial DNA
mTOR	Mammalian target of rapamycin
mTORC1	Mammalian target of rapamycin complex 1
mTORC2	Mammalian target of rapamycin complex 2
Myt1	Cdk1 inhibitory kinase
MZT	Maternal zygotic transition
NPPC	Natriuretic peptide precursor C
PABP	Poly(A)-binding protein
PAP	Poly(A) polymerase
PB	Polar body
PB1	First polar body
PB2	Second polar body
PI	Prophase 1
PI3K	Phosphoinositide 3-kinases
PKA	Protein kinase A
PMSG	Pregnant Mare Serum Albumin
PVS	Perivitelline space
S6K1	p70S6 kinase 1
TERT	Telomerase reverse enzyme
TGF-β	Transforming growth factor beta
TOS	Total oocyte scoring
Tsc1/Tsc2	Tumor suppressor complex
Wee1	Nuclear kinase belonging to the Ser/Thr family of protein kinases

ZP	Zona pellucida

ABSTRACT

Obaideen, M. (2022). Detection of *c-Abl* Tyrosine Kinase and The Mammalian Target of Rapamycin (*mTOR*) Regulation in Mouse Oocyte Maturation. Yeditepe University, Institute of Health Sciences, Master Thesis. İstanbul

In this thesis, we aimed to investigate the roles of *mTOR* and *c-Abl* and the relationship between them during the process of oocyte maturation which includes Prophase I (PI), Metaphase I (MI), and Metaphase II (MII) stages of oocyte development. We collected GV oocytes from mouse ovaries and then treated them with imatinib (1 μM, 5 μM and 10 μM) which is a *c-Abl* inhibitor and rapamycin (1000 μM) which is an mTORC1 inhibitor for 16 hr. We then evaluated the developmental potential of GV oocytes to MII stage. We recorded the rate of GV, MI and MII oocytes after the culture period and scored them. We also evaluated mRNA levels of *mTOR* and *c-Abl* with qRT-PCR in GV, MI and MII oocyte stages in all experimental groups. According to our findings, Rapamycin had a slightly positive effect on the rate of oocyte maturation while it had a slightly negative effect on the oocyte morphology. On the contrary (Interestingly), the mRNA expression of *mTOR* in GV, MI and MII oocytes in the rapamycin group did not decrease. Imatinib had a negative effect on both oocyte maturation and morphology in a dose-dependent manner. While 1 μM imatinib had a slightly negative effect, 10 μM imatinib had a greater negative effect on the rate of oocyte maturation and morphology. mRNA expression levels of *c-Abl* in GV and MII significantly decreased in 1 μM and 5 μM imatinib treatment groups. The qRT-PCR results that compared the mRNA expression levels of *c-Abl* and *mTOR* in the GV, MI and MII oocytes in all experimental groups showed that *c-Abl* inhibition led to an increase in *mTOR* expression. In this thesis, we suggest that mTOR and *c-Abl* may have important roles in oocyte maturation. Moreover, we have shown that *c-Abl* inhibition leads to an increase in *mTOR* activity. In conclusion, understanding the roles of c-Abl and mTOR during oocyte maturation will help us improve oocyte and embryo quality and also will provide new insights into mechanisms underlying the regulation of oocyte maturation.

Key words: c-Abl, mTOR, oocyte maturation, mouse.

ÖZET

Obaideen, M. (2022). Fare Oosit Maturasyonunda *c-Abl* Tirozin Kinaz ve Memeli Rapamisin Hedefi (*mTOR*) Düzenlenmesinin Belirlenmesi. Yeditepe Üniversitesi, Sağlık Bilimleri Enstitüsü, Master Tezi. İstanbul

Bu tez çalışmasında, oosit gelişiminin Profaz I (PI), Metafaz I (MI) ve Metafaz II (MII) aşamalarını içeren oosit olgunlaşma sürecinde *mTOR* ve *c-Abl*'in rollerini ve mTOR ile c-Abl arasındaki ilişkiyi araştırmayı amaçladık. GV aşamasındaki oositler fare ovaryum dokusundan izole edilerek, *c-Abl* inhibitörü olan imatinib (1 μM, 5 μM ve 10 μM) ve mTORC1 inhibitörü olan rapamisin (1000 μM) ile 16-18 saat inkübe edildi. Oosit kültürü sonrası GV, MI ve MII oranlarını kaydettik ve oositleri skorladık. Ayrıca tüm deney gruplarında kültür sonrasında GV ve MI aşamasında duraklayan oositler ile MII aşamasındaki oositlerde *mTOR* ve *c-Abl* ekspresyonunu qRT-PCR yöntemi ile mRNA düzeyinde belirledik. Rapamisinin, oosit olgunlaşmasını hızlandırdığını ancak oosit morfolojisi üzerinde olumsuz bir etkiye sahip olduğunu gözlemledik. 1 μM imatinib uygulamasının, oositin olgunlaşması ve morfolojisi üzerinde olumsuz bir etkiye sahip olduğunu belirledik. 5 μM imatinib uygulamasının, oosit olgunlaşması ve oosit morfolojisi üzerinde olumsuz bir etkiye sahip olduğunu gözlemledik. 10 μM imatinib uygulamasının, oosit olgunlaşması ve oosit morfolojisi üzerinde büyük ölçüde olumsuz bir etkiye sahip olduğunu değerlendirdik. 1 μM ve 5 μM imatinib tedavi gruplarında *c-Abl* ekspresyonunun GV ve MII'de aşamasındaki oositlerde önemli ölçüde azaldığı belirlendi. *c-Abl* ve *mTOR* ekspresyonunu tüm deney gruplarında GV, MI ve MII aşamasındaki oositlerde değerlendirdiğimizde, c-Abl'i inhibisyonu sonucu *mTOR* ekspresyonun arttığını belirledik. Tez çalışmamızın sonucunda, mTOR ve c-Abl'in oosit olgunlaşmasında önemli rollere sahip olabileceğini ve c-Abl ile mTOR arasındaki ilişki neticesinde c-Abl inhibisyonunun mTOR ekspresyonunun artmasına neden olabileceğini belirledik. Sonuç olarak, oosit olgunlaşması sürecinde c-Abl ve mTOR'un rollerinin ortaya koyulması, oosit ve embriyo kalitesini iyileştirmemize yardımcı olacağını ve ayrıca oosit olgunlaşmasının düzenlenmesi sürecinde görev alan mekanizmalar hakkında yeni bilgiler sağlayacağını düşünmekteyiz.

Anahtar Kelimeler: c-Abl, mTOR, oosit olgunlaşmas, fare

1. INTRODUCTION and PURPOSE

In the ovarian cortex, there are huge numbers of primordial follicles that begin to form during the embryonic stage. Their numbers in the fifth month reach a peak where it becomes 7 million, then decreases until 400 thousand at birth and then eventually to 40 thousand at puberty. In every ovarian cycle, one egg undergoes maturation and the others are subjected to atresia until the stock runs out and the female enters menopause[1]. Many scientists have been working to reduce the rate at which a woman's fertility deteriorates due to aging. However, scientific research has confirmed that the goal at present is not limited to preserving the stock of follicles, but rather to obtaining a high-quality mature egg that leads to a healthy fetus and increases the chance of implantation and the continuation of pregnancy[2,3].

During the life of the oocyte, a set of complex, interconnected and simultaneous nuclear, cytoplasmic and epigenetic developments take place that supports each other and lead to the production of a mature egg that possesses all the biological characteristics to form a healthy fetus. This developmental period is called oocyte maturation[4,5]. In the embryonic stage, the primordial follicles are arrested in the prophase stage of the first meiosis and remain dormant until adulthood [6]. At the beginning of each ovarian cycle, the primordial follicles grow and reach the antral stage, and then their first meiosis resumes under the influence of the luteinizing hormone (LH), where the germinal vesicle (GV) collapses, the polar body (PB) emerges and a haploid oocyte forms that enter into the second meiosis[7-11]. In conjunction with these events, cytoplasmic organelles proliferate and change places of their distribution (such as mitochondria and endoplasmic reticulum) to raise the level of energy needed for growth and to fold the increased proteins, and actin filaments build the appropriate cytoskeleton to coordinate spindle movement and orientation, chromosome segregation and other dynamic processes needed to resume meiosis[4,12-15]. Cytoplasmic molecular maturation also occurs as the maternal messenger ribonucleic acid (mRNA) becomes active and exits the nucleus and synthesizes proteins needed for meiotic maturation[16-19]. Epigenetic mechanisms such as DNA methylation and acetylation of histones control gene expression and the regulation of transcription processes during development[4,20,21].

The mammalian target of rapamycin (*mTOR*) is a serine/threonine-protein kinase that plays a role in primordial follicle maturation, somatic cell proliferation and differentiation, supports meiotic maturation by enhancing transcription, translation and

control of the actin cytoskeleton and maintains a balance between primordial follicle activation and dormancy[22-27]. The absence of mTOR negatively affects the maturation of primordial follicles, it may lead to the death of a large number of follicles or the maturation of defective follicles, deformed spindles, translation defects, asymmetric chromosome segregation, DNA damage, and immature somatic cells. It was observed that inhibition of mTOR by Rapamycin in vitro, prevented follicle growth and led to the appearance of oocyte-free follicles[28].

Abelson tyrosine kinase (*c-Abl*) is a non-receptor tyrosine kinase that plays a role in oocyte growth, meiotic division, repair of DNA damage, activation of transcription proteins and promoting meiotic maturation through regulation of the actin cytoskeleton[29,30]. Inhibition of *c-Abl* by imatinib leads to the death of follicles or the development of defective oocytes[31]. Also, *c-Abl* regulates telomerase function and proliferation in granulosa cells and Imatinib leads to granulosa cell apoptosis[32,33].

A study suggested a possible interaction between tumor protein (p53) and mTOR is the tyrosine kinase *c-Abl*, which interacts with p53 and phosphorylates mTOR on tyrosine residues[34]. *c-Abl* inhibits the kinase activity of *mTOR*. Since c-Abl is activated by ionizing radiation and certain other DNA-damaging agents, these data suggest that *c-Abl* may provide a link between DNA damage and impairment of *mTOR* signaling leading to dephosphorylation of eukaryotic translation initiation factor 4E-binding protein 1 (4E-BP1) and increased binding to eukaryotic translation initiation factor 4E (eIF4E)[35].

In the light of literature, we hypothesized that the association between *c-Abl* and *mTOR* may be very important during mouse oocyte maturation. Therefore, in this thesis study, we aimed to evaluate the roles and possible interaction of *mTOR* and *c-Abl* tyrosine kinase during mouse oocyte maturation which includes Prophase I (PI), and Metaphase I (MI) and Metaphase II (MII) stages of oocyte development.

2. LITERATURE REVIEW

2.1. Ovary and Folliculogenesis

2.1.1. Structure of Ovary

The ovaries are almond-like female genital glands, the size of a thumb's finger, about four centimeters in length, located in an area called the ovarian fossa and they are connected to the fallopian tubes[36,37]. They are held in place by ligaments that connect to the uterus and the wall of the pelvis[38]. These two ovaries are responsible for the production of eggs and female sex hormones, such as estrogen, which is secreted from the follicle, and progesterone, which is secreted from the yellow body[37]. The ovary consists of the cortex and medulla. The cortex is a thin, superficial white layer, that generates eggs, containing stromal cells and thousands of primordial follicles and the medulla is the largest part of the ovary, as it is located in its center, and is rich in blood vessels that are placed between muscle connective tissue[39]. The surface of the ovary is surrounded by germinal epithelium made of cubic epithelial cells on the outside. Between the germinal epithelium and cortex is the tunica albuginea, a tight connective tissue layer (Figure 2.1.1)[36]. Before puberty, the surface of the ovarian tissue is smooth due to the absence of mature follicles, but after puberty and repeated ovulation, the surface of the ovary becomes roughly wavy due to the scars and corpus luteum left by the Graafian follicles after ovulation[37].

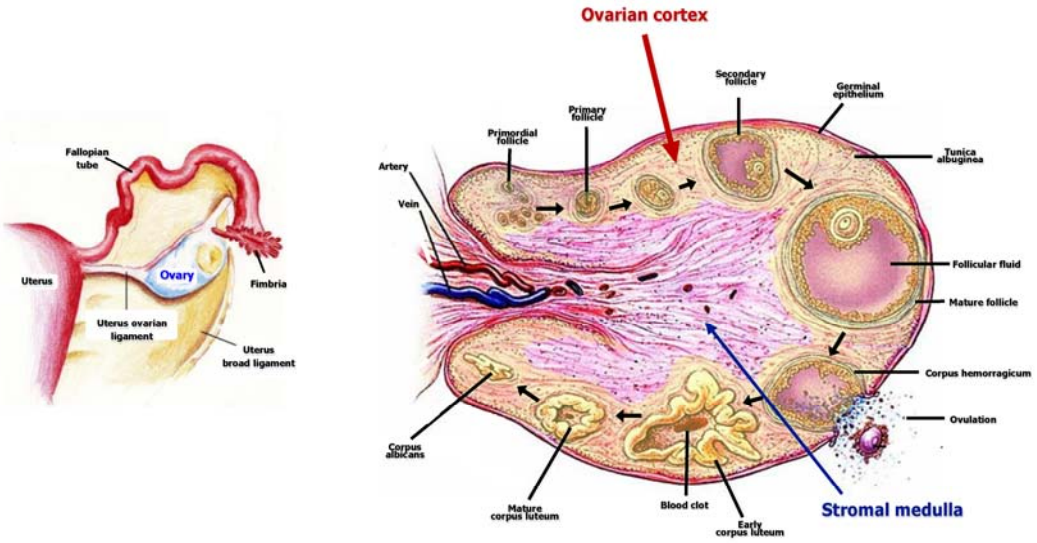

Figure 2.1.1. Anatomic location and structure of the ovarian tissue including cortical components[40].

2.1.2. Folliculogenesis

This process ensures the formation of the female reproductive cell (oocyte) from its emergence to full maturity. This formation starts from the embryonic stage until adulthood and it lasts for several months in animals and tens of years in humans. The oocyte is formed as follows: Primordial germ cells migrate from the yolk sac during the embryonic stage, colonizing the genital ridges. If the embryo is female (XX), the genital ridges differentiate into an ovary and those cells turn into oogonia[41]. Oogonia proliferate by mitotic division, forming millions of primary oocytes[42]. Epithelial cells also proliferate and surround them, forming a layer of squamous cells. The primary oocytes with the layer of squamous epithelial cells surrounding them are called the primordial follicle[43]. Most primary oocytes do not undergo meiosis due to atresia[2]. In puberty, 15-20 primordial follicles begin to develop in each ovarian cycle, but only one of them matures. Primordial follicles turn into primary follicles as a result of the increase in the size of the egg and the transformation of the squamous cells surrounding the egg into cuboidal cells, under the influence of the follicle-stimulating hormone (FSH)[44,45]. Cubic cells proliferate and turn into granulosa cells. Both the granulosa cells and primary oocyte secrete extracellular glycoproteins that surround the oocyte and form the zona pellucida (ZP). As the follicle continues to grow, the somatic cells surrounding the oocyte

differentiate and organize into theca interna on the inside consisting of secretory cells, and theca externa on the outside is a fibrous capsule. Then the follicular fluid is secreted from the granulosa cells and this fluid collects in the form of vacuoles so this follicle is called a secondary follicle or preantral follicle. Then the secondary follicle matures under the influence of LH and begins the pre-ovulatory growth phase. First meiosis is completed and secondary oocyte and fisrt polar body (PBI) are formed. The vacuoles join together to form a single vacuole called the cavity antrum, so the mature follicle is also called the antral follicle[45]. The first row of granulosa cells surrounding the oocyte is called corona radiata and the second row is called Cumulus oophorous. The secondary oocyte enters the second meiotic division, but it stops in the metaphase stage three hours before ovulation and don't complete its meiotic division unless fertilization occurres (Figure 2.1.2)[44].

During folliculogenesis, follicle growth undergoes a delicately balanced process between levels of hormones secreted from the hypothalamus and hormones secreted by follicle cells that stimulate and inhibit each other periodically[38]. The maturation of the oocyte in the antral stage is regulated by FSH and LH in addition to growth factors such as transforming growth factor-beta (TGF-β). Whereas, FSH receptors are found in granulosa cells that initially produce the estrogen hormone needed for the maturation of the developing dominant follicle. LH is responsible for inducing ovulation, resumption of first meiosis, and the production of progesterone, estrogen and androgen required for oocyte maturation[2,44-46]. As for the preantral follicle, it grows dependent on growth factors such as growth hormone (GH) and insulin-like growth factor (IGF) and on the gap junctions that allow the passage of nutrients between the granulosa cells and the primary oocyte[44,47,48].

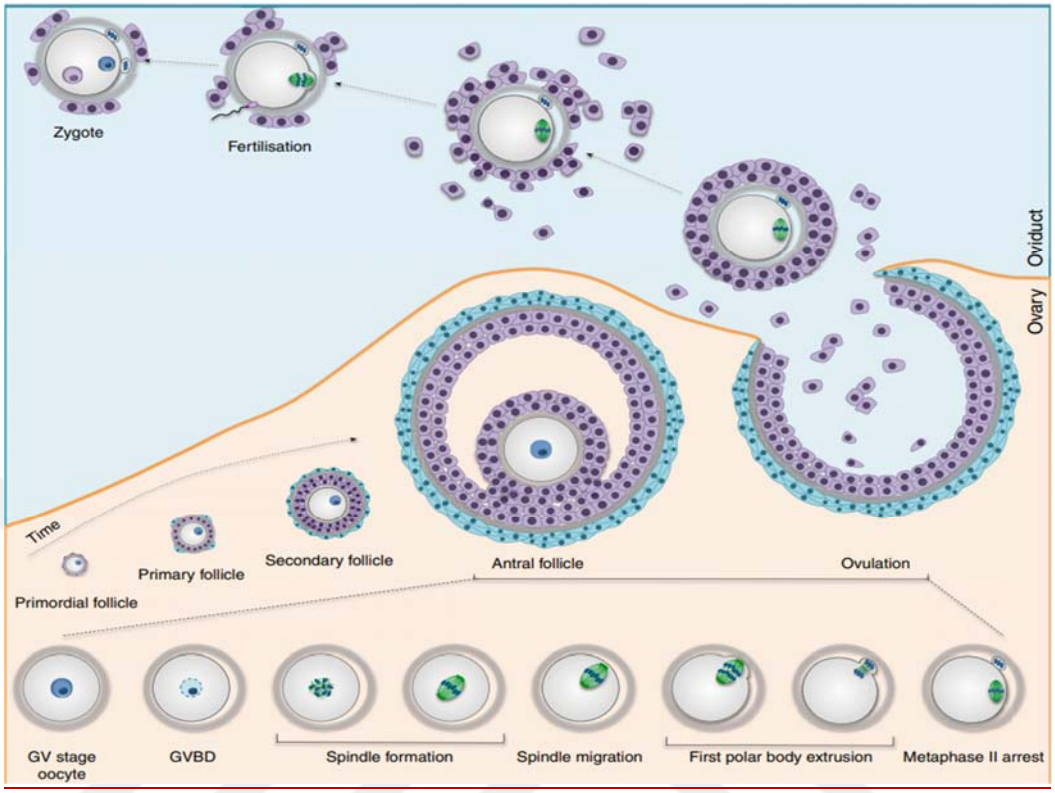

Figure 2.1.2. The oocyte's journey to fertilisation[49].

2.1.2.1. Oocyte Morphology

In in vitro fertilization (IVF) centers, specialists not only stimulate the eggs but also evaluate the quality of the eggs, not only by examining the integrity of the chromosomes but through the morphological parameters, which allow us to predict the degree of oocyte efficiency. The higher the oocyte quality, the more likely to have a healthy embryo capable of implantation.

An ideal mature human oocyte contains a transparent cytoplasm of a normal shape, a single PB, a transparent outer layer of medium thickness (ZP) and a normal perivitelline space (PVS) (Figure 2.1.2.1.A). The medium-quality oocytes have a mildly abnormal shape, mildly granular cytoplasm, an abnormal or segmented PB, slightly thick ZP and big or small PVS. As for the poor quality oocyte, it is characterized by an abnormal shape, deformed or granular cytoplasm, an abnormal or segmented PB, thick and dark ZP, big size of PVS and the presence of vacuoles, refractive bodies and smooth

endoplasmic reticulum (SER)[50,51]. There may also be an increase in the proportion of defective mitochondria in oocytes of older mothers (Figure 2.1.2.1. B-C-D-E-F-G-H)[52,53].

MS fibers are groups of filaments that stick out from the centrioles. This spindle can deconstruct replicated DNA during meiosis and attract one copy towards each pole, thus reducing the incidence of aneuploidy or daughter cells that contain incomplete sets of chromosomes. Therefore, the integrity of the spindle expresses the degree of efficiency of the oocyte and can be considered one of the most important morphological parameters of the oocyte[54].

Also, the large oocyte suggests the presence of chromosomal abnormalities, and such an oocyte is called a giant oocyte (Figure 2.1.2.1.I)[55]. In some oocytes, the location of the MS may deviate from the PB, but this deviation is not significant, unless the angle of deviation is larger than 90%, it will lead to abnormalities in the zygote after fertilization[53,56].

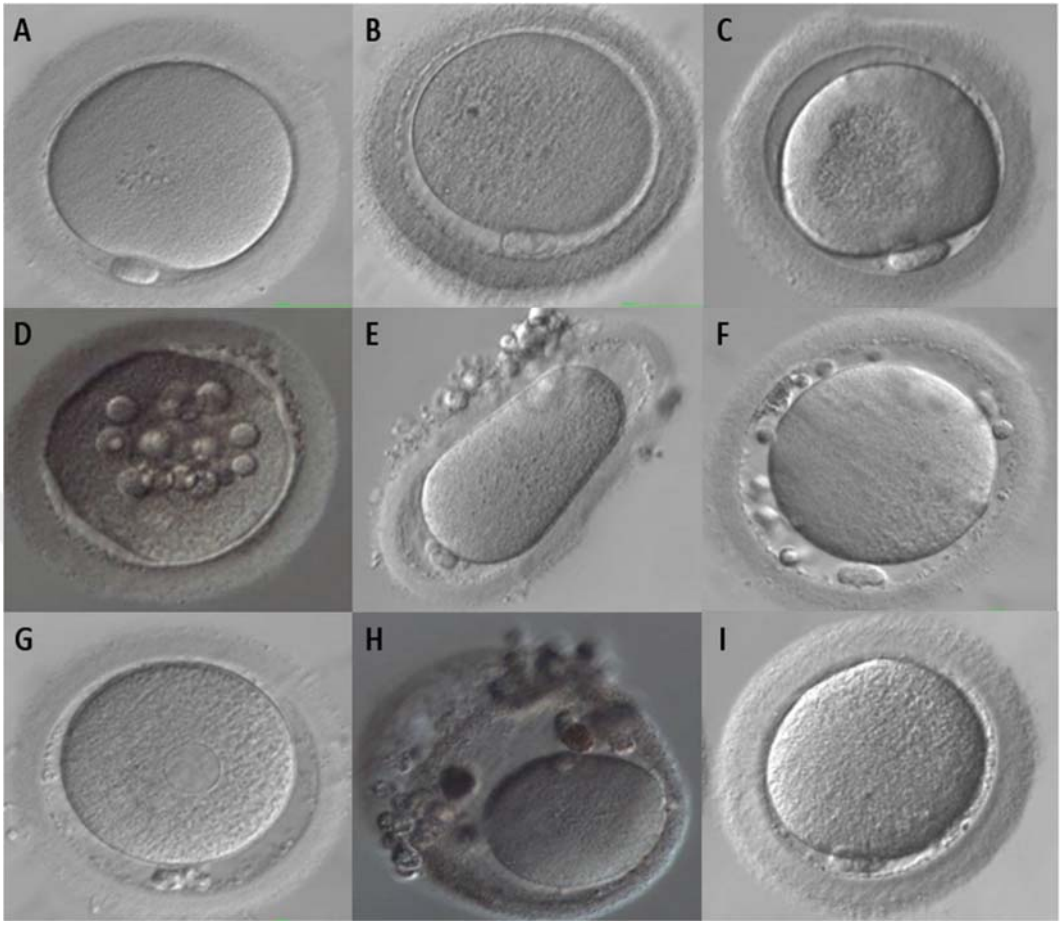

Figure 2.1.2.1. (A) Oocyte with normal cytoplasm. (B) MII oocyte with granular. ZP is thicker in the lower-left part of the oocyte. (C) MII oocyte showing organelle clustering forming a large centrally located granular area in the cytoplasm. ZP has an irregular shape. (D) Vacuolated oocyte. Depicts an oocyte with several small vacuoles distributed throughout the oocyte cytoplasm. (E) Ovoid MII oocyte. Note the ZP is also ovoid in appearance and the PVS is enlarged at both poles. (F) MII oocyte with a fragmented PBI and several cellular fragments within the PVS which are almost indistinguishable from PB1. (G) MII oocyte showing plaques of dilated SER discs in the cytoplasm. The PVS is enlarged and PB1 is fragmented. (H) Elongated MII oocyte within a grossly distended and irregular ZP. (I) Giant oocyte[53].

2.1.2.2. Oocyte Maturation

Oocyte maturation is a series of simultaneous nuclear, cytoplasmic and epigenetic changes that bring one of the primordial follicles every month to the stage of fully mature

and prepare it for fertilization[4,8]. This process takes about 14 days during which a primordial follicle develops into an antral follicle, and in response to the LH, resumes its meiosis I (MI) from the diplotene stage arrest that had begun almost before birth, leading to the breakdown of the germinal vesicle (GV), MS formation, extrusion of the PBI, rearrangement of the cortical cytoskeleton, and the entry into the meiosis II (MII). Thus, a haploid oocyte is formed but arrests at the metaphase of MII until fertilization (Figure 2.1.2.2)[8-11,57].

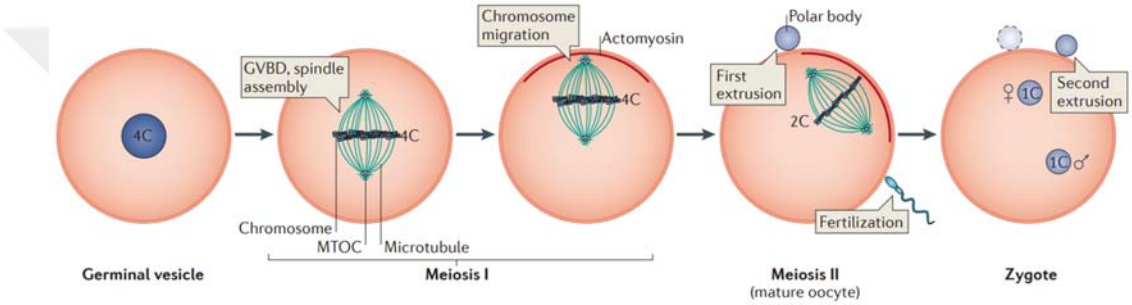

Figure 2.1.2.2. Simultaneous coordination between nuclear and cytoplasmic processes during the maturation of a mammalian oocyte[58].

Cumulus cells and mural granulosa cells participate in the oocyte maturation process through the gap junction communication and their secretion of substances needed for oocyte maturation in response to gonadotropins, and also they play a role in resumption meiosis I by inhibiting maturation promoting factor (MPF)[57-60].

2.3. Oocyte Nuclear Maturation

The primordial follicle contains 46 chromosomes and therefore must undergo meiotic divisions in order for the number of chromosomes to remain constant and for genetic diversity to occur among the offspring.

2.3.1. Meiotic Division

Meiosis is the process of reducing the number of chromosomes in half in order to form haploid gametes capable of fertilization and this is done in synchronization and in association with the process of cytoplasmic maturation[10,15]. Oogonia are diploid cells that

enter the prophase stage of the first meiotic division in which the chromosomes which have been duplicated in the previous phase of the interphase of the cell division appear as long, slender filaments. This early stage of prophase is called leptotene. Then they enter into the zygotene stage, in which the homologous chromosomes close together, and form synapses. Then the crossing-over, which is known as chiasma, occurs in the pachytene stage[23,61]. Then begins the diplotene stage, in which the bivalents (pair of homologous chromosomes) separate from each other, except for the chiasma region. All oocytes are arrested at this stage as primordial follicles until adulthood. During each ovarian cycle, several primordial follicles begin to grow under the influence of FSH, but only one of them can reach the antral follicle, while the others degenerate and turn into atretic follicles[2,44,45]. According to the sudden LH surge, at the end of the ovarian cycle, the antral follicle resumes the meiosis I and enters to diakinesis stage, in which the chiasma regions begin to terminalize, the nucleolus begins to disappear, the GV breaks down, and the MS forms[8,9,49,59]. The primordial follicle enters the metaphase stage and the bivalent line up at the spindle equator. Then, in the anaphase stage, homologous chromosomes separate from each other and migrate to each pole different from the other. Then follicle enters into the telophase stage, and the nuclear membrane is formed around each group of chromosomes and the cytoplasm is divided unevenly, resulting in two daughter cells, one of which is very small and has little cytoplasm, it is PBI, and the other is large that takes up almost all the cytoplasm, it is the secondary oocyte that directly enters into the second meiosis that arrests in the metaphase stage until fertilization. Upon fertilization, the oocyte resumes its second meiosis, becomes haploid as the sister chromosomes separate, and the second polar body (PB2) extrudes. Then the male and female nuclei unite, and the mitotic divisions of the embryo begin (Figure 2.3.1)[49,59,62,63].

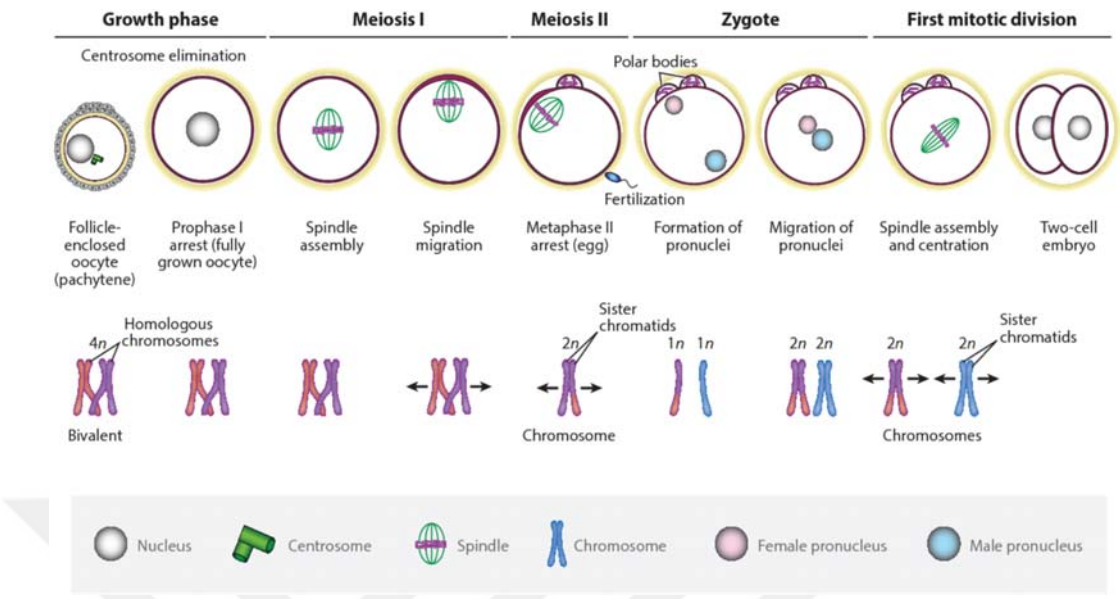

Figure 2.3.1. Oocyte meiotic divisions and early egg development[63].

2.3.1.1. Regulation of Meiotic Arrest of Oocytes at Prophase I Stage

In mammalian oocytes, mural granulosa cells, cumulus cells, gap junction communication, cyclic adenosine monophosphate (cAMP) levels, and MPF activity status play the main role in oocyte arrest in the diplotene stage of meiosis I. This arrest is believed to be very important because it gives the sister chromatids enough time to repair each other from the genetic damages[64,65].

When the G protein-coupled receptor 3 (GPR3), which is located on the membrane of the primary oocyte in the primordial follicle, is activated by an unknown promoter, it binds to G proteins that stimulate adenylate cyclase (AC). This increases cAMP production which in turn increases protein kinase A (PKA) activity that inhibits Cdc25B phosphatase and activates Wee1/Myt1 kinase. The activation of Wee1/Myt1 kinase inhibits the MPF by phosphorylating one of its subunits (CDK1) and transporting it to the cytoplasm, which leads to arresting of meiosis I at the stage of diplotene[6-8,10,66].

Mural granulosa cells and cumulus cells contribute to maintaining this arrest in the preovulatory follicle, as granulosa cells produce more cAMP and transfer it to the oocyte, and also produce natriuretic peptide precursor C (NPPC) and transfer it to the cumulus cells. NPPC converts guanosine-5'-triphosphate (GTP) to cyclic guanosine monophosphate (cGMP) which is also transported to the oocyte through gap junctions

and inhibits cyclic adenosine monophosphate- phosphodiesterase (cAMP-PDE), this leads to increased accumulation of cAMP in the oocyte[57,59]. FSH also plays a role in maintaining this arrest by increasing the production of NPPC in the granulosa cells, which means an increase in the production of cAMP in the oocyte (Figure 2.3.1.1.a)[8,67].

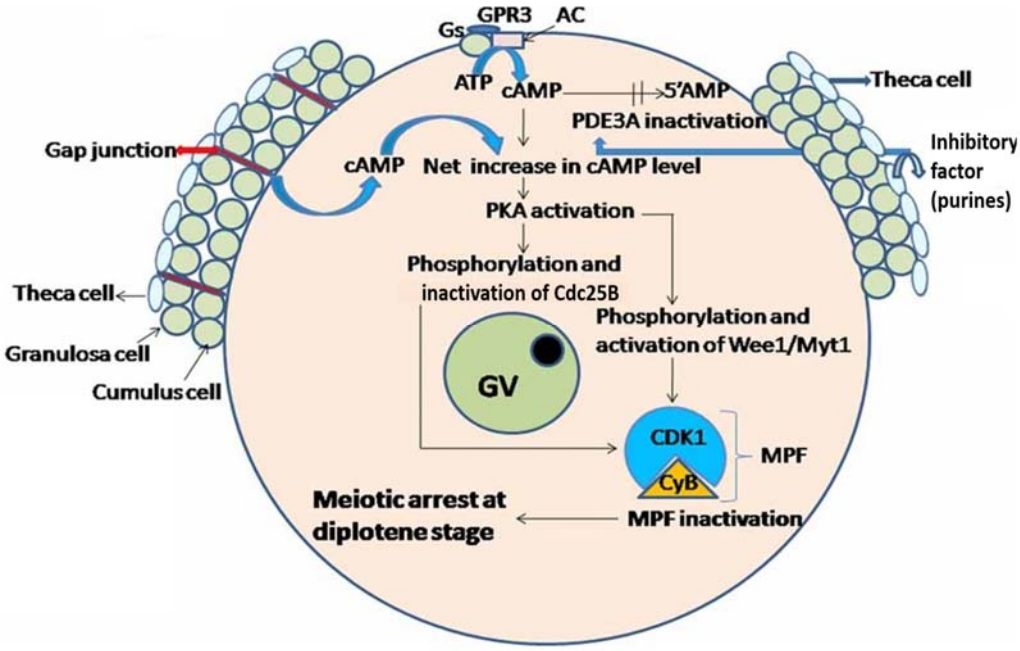

Figure 2.3.1.1 (a). A proposed model for the maintenance of meiotic arrest at the diplotene stage in preovulatory follicle[57].

At the end of the ovarian cycle, the LH surge leads to the resumption of the first meiosis. Its mechanism is still not fully understood, but it is clear that it does so by disrupting the gap junctions and activiting cAMP-PDE, leading to lowering the cAMP level and thus reactivating the MPF. Studies have shown that LH increases the level of cAMP in granulosa cells, which either activates the epidermal growth factor (EGF)-like factors in the cumulus cells, leading to the disruption of the gap junctions and thus reactivation of the cAMP-PDE and lowering the cAMP level, or it inhibits NPPC and prevents the production of cGMP, this leads to reactivation of the cAMP-PDE and thus reactivation of the MPF that is transported to the nucleus, causing the breakdown of GV and resumption of meiosis I from diplotene arrest (Figure 2.3.1.1.b)[8,57,59,68].

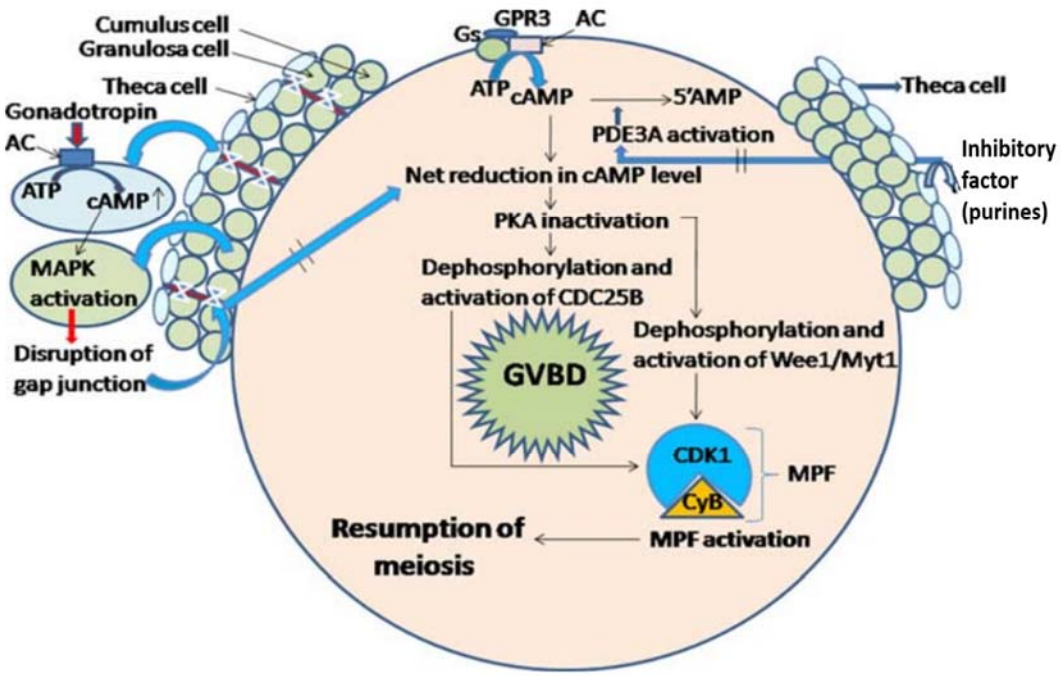

Figure 2.3.1.1 (b). A proposed model for LH-induced meiotic resumption in follicular oocyte[57].

2.3.1.2. Regulation of Meiotic Arrest of Oocytes at Metaphase II Stage

The arrest at the metaphase stage of second meiosis in the secondary oocyte depends on the c-MOS/MEK/MAPK pathway, which plays the main role in activating the cytostatic factor that stimulates MPF stabilization and spindle stability that are essential to initiate and continue this arrest which will continue until fertilization. The c-MOS/MEK/MAPK pathway stimulates one of the components of the cytostatic factor, known as emi2, which in turn inhibits the APC/C by Cdc20, thus stabilizing the MPF (Figure 2.3.1.2)[2,57,69].

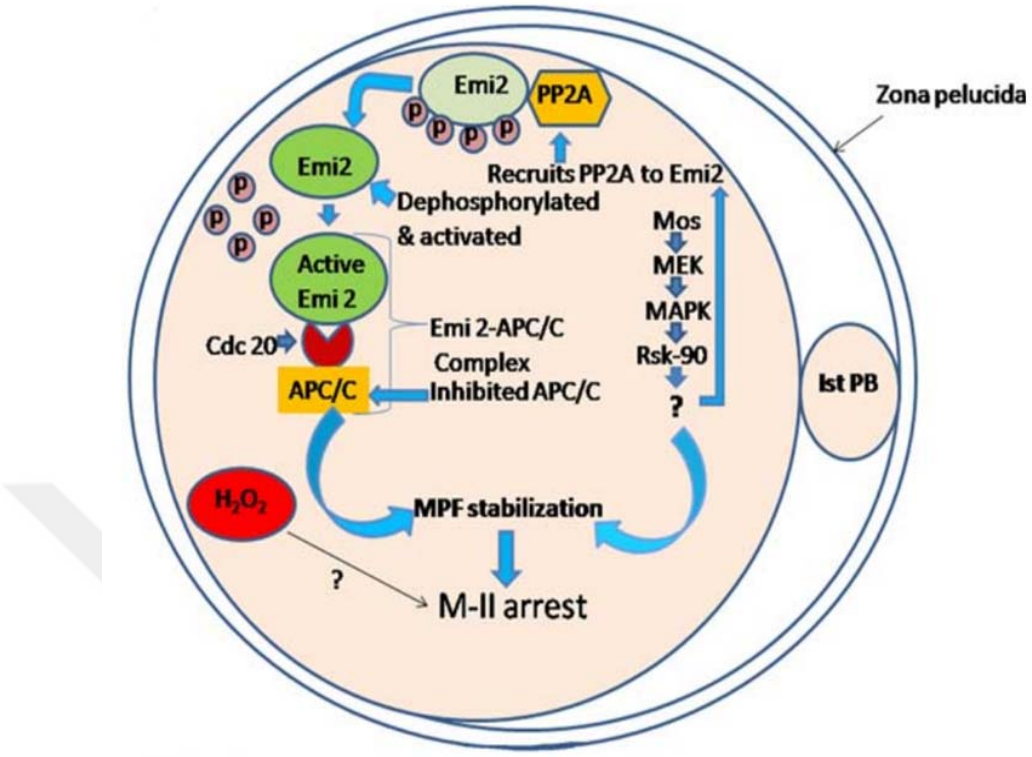

Figure 2.3.1.2. A proposed model for maintenance of meiotic arrest at M-II stage[57].

When fertilization occurs, calcium production increases in the oocyte, which leads to stimulation of Ca^{2+}/calmodulin-dependent protein kinase II (CAMKII), which restores emi2 phosphorylation and thus activates APC/C, leading to the resumption of the meiosis II and the offspring of the PB2[2,57,69].

2.4. Oocyte Cytoplasmic Maturation

Cytoplasmic maturation is part of the oocyte maturation process. It accompanies nuclear maturation and contributes to the production of haploid oocytes with high developmental efficiency and capable of undergoing fertilization[15,70]. Cytoplasmic maturation includes a set of molecular and structural changes and modifications that occur in the cytoplasmic organelles before the emergence of the PB[4,15]. These cytoplasmic changes play a decisive role in completing nuclear maturation, as they activate the pathways required for the oocyte to exit from the arrest of the PI and enter the MII. Also, oocyte quality can be predicted by the morphology of cytoplasmic organelles, which reflects the degree of maturation and efficiency of the oocyte[60,71]. Cytoplasmic maturation

divides into two parts: cytoplasmic organelle maturation and cytoplasmic molecular maturation[5].

2.4.1. Oocyte Cytoplasmic Organelle Maturation

During oocyte maturation and resumption of the first meiosis, organelle changes occur in the mitochondria, ribosomes, ER, cortical granules, and the Golgi complex[72]. Mitochondria provide the energy required for the vital processes during the development of oocytes, and their number is proportional to the need for that energy. Thousands of them are formed in the primordial germ cells (PGCs) and then multiply by fission with the development of the follicle and reach a peak in the GV stage where the GV collapses, the MS forms, the chromosomes separate, and then their number decreases in the mature oocyte by fusion (two mitochondria join to form a single mitochondrion). The mitochondria also change their location according to the severity of the energy need. Before the germinal vesicle breakdown (GVBD), the mitochondria are lined up around the membrane of the nucleus. After the GVBD, they are located around the MS, in the metaphase stage they accumulate around the equatorial plate to support the chromosomal separation, and after the emergence of the PB, they scatter into the cytoplasm[1,15,72,73]. The number of mitochondrial DNA (mtDNA) increases as maturation increases and is an important marker for determining oocyte quality. Studies have proven that defects in the function of mitochondria lead to abnormalities in genes, as it was found that mitochondria prevent chromosomal translocations and thus contribute to maintaining the integrity of the genome[12]. Mitochondria also regulate maternal epigenetics. Mitochondrial metabolites act as inhibitors or cofactors of the activity of key enzymes involved in the process of acetylation and methylation of histones and DNA. The number of mtDNA copies affects these metabolites and therefore maternal epigenetics, which reflects the importance of mtDNA number[13].

The endoplasmic reticulum (ER) plays an important unique role during oocyte maturation, especially in the stage of meiosis II. In GV, ER localizes in cortical regions. After GVBD, it spreads throughout the oocyte, especially around the MS, and upon fertilization occurs, it releases large amounts of calcium through the Inositol trisphosphate (IP3), which stimulates the resumption of meiosis II, the formation of the nucleus and the extrusion of the PB2. They also fold proteins, metabolize fats, and rid the egg of excess toxins during growth[5,71,74,75].

The Golgi apparatus is attached to MS microtubules that fragment it into mini-Golgis when meiotic divisions occur. Mini-Golgis are scattered throughout the cytoplasm and the fragmentation state continues until it almost disappears from the mature oocyte[4,5,71].

In GV, cortical granules are uniformly distributed throughout the cytoplasm. After GVBD, they are lined up under the oolemma. The cytoskeleton is a network of filaments and microtubules that extend from the nucleus to the cell membrane and regulate the movement of mitochondria, ER and cortical granules during oocyte maturation. Also during meiosis, microtubules form MS, and actin filaments line up under the cortex and around chromosomes, causing chromosomal movement, MS migration, MS rotation and PB extrusion. In GV oocytes, intermediate filaments assemble into large cortical aggregates. In metaphase, I, scatter into small pieces and then spread evenly throughout the cytoplasm in metaphase II (Figure 2.4.1)[4,14,76].

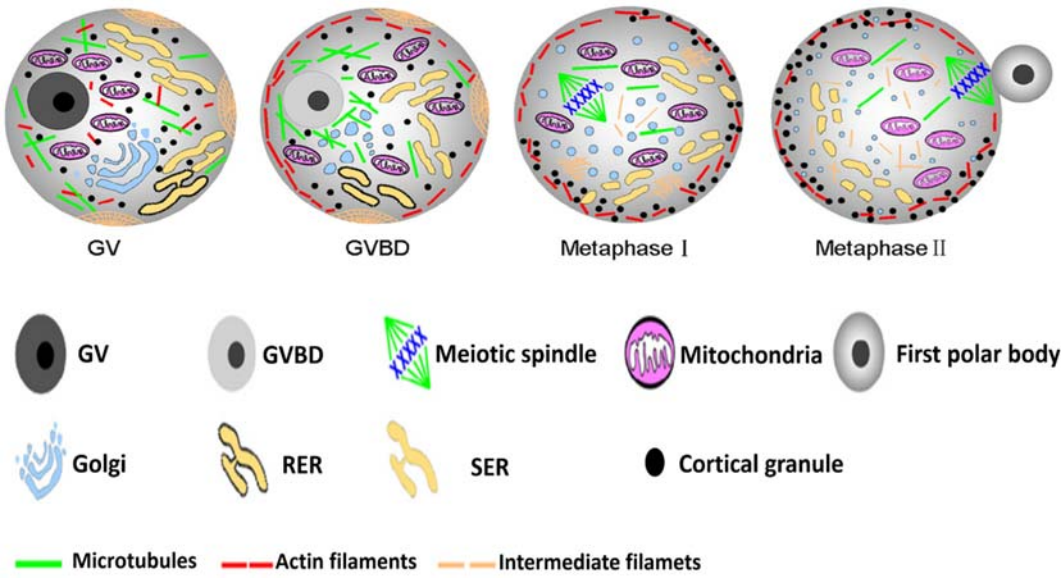

Figure 2.4.1. Distribution of cytoplasmic organelles and the cytoskeleton during oocyte maturation in mouse[76].

2.4.2. Oocyte Cytoplasmic Molecular Maturation

Meiotic maturation depends on maternal mRNA proteins, whose synthesis begins after GVBD. During follicle development, mRNA transcripts are produced and stored

which remain silent (dormant) until first meiosis resumes. After GVBD, the dormant mRNA is activated by cytoplasmic polyadenylation (CP), where a poly(A) tail is added to the mRNA allowing it to exit from the nucleus and translate it into proteins that contribute to the formation of the MS and maintain the stability of the second arrest. Cytoplasmic polyadenylation element-binding protein (CPEB) is the first key factor that plays a role in storing dormant mRNA transcripts and then activating their translation. In the GV stage, CPEB binds to a Maskin protein that binds to eIF4E, forming a loop between the terminal of mRNA, which impedes the binding of translation initiation factors. Also, CPEB binds poly(A) polymerase (PAP). This process is called translation suppression. After the resumption of the first meiosis, Extracellular signal-regulated kinases (ERK1/2) phosphorylate CPEB which recruits the cleavage and polyadenylation specificity factor (CPSF) and PAP, that builds the poly(A) tail. CPEB phosphorylation also results in its dissociation from a poly(A)-binding protein (PABP) that binds a poly tail (A) to eukaryotic translation initiation factor 4G (eIF4G) which leads to the dissociation of the loop, enabling the interaction of translation initiation factors, causing resuming of translation (Figure 2.4.2)[16,77].

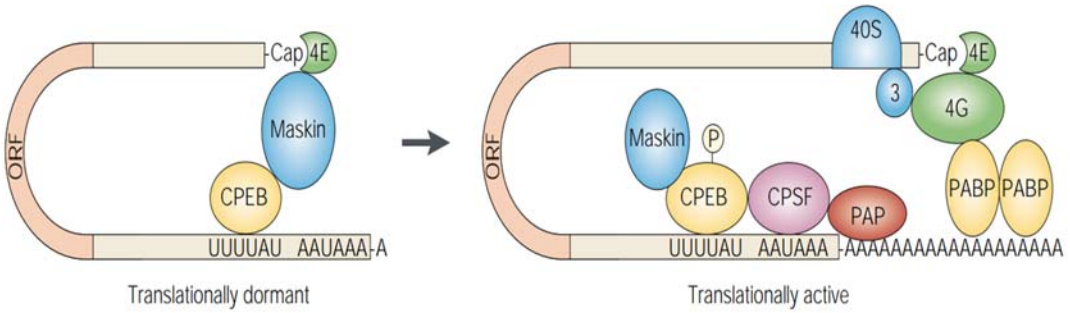

Figure 2.4.2. CPEB-mediated translational control in immature oocyte messenger mRNAs containing a cytoplasmic[77].

During meiotic maturation, Poly (A) RNA is localized, as a cloud form, around the GV and then around the MS and microtubules, ensuring the synthesis of more efficient and active local proteins than transported proteins[17].

Translation of the stored maternal mRNA continues until 4 cell stage -in humans- and the two-cell stage -in mice- of the zygote cleavage. This leads to the deterioration and death of the mRNA transcripts and the start of transcription of the zygote genome (the genome of the father and mother together). Thus, the development of the fetus moves from dependence on the mother's genome to dependence on the zygote genome, which is called Maternal to zygotic transition (MZT)[5,18,19].

2.5. Oocyte Epigenetic Maturation

During the maturation of the oocytes, changes in the pattern of gene expression occur at several stages of development, such as arresting transcription at GVBD and activating transcription after fertilization. Epigenetic mechanisms program this arrest and activation at the appropriate time and determine the working genes and the silent genes, this process is called epigenetic maturation[5,20]. Among the most important of these epigenetic mechanisms are DNA methylation, acetylation of histones, and modification of histones. In the growing follicle stage, histone deacetylation occurs, which increases the chromatin density, thus preventing the binding of transcription factors to the DNA. Also at this stage, the DNA methylation process begins, as a methyl group is added at the 5-carbon of the cytosine ring, leading to suppression of transcription. After fertilization, the histones are acetylated, which leads to chromatin unfolding, thus allowing transcription factors to enter the DNA and the resumption of transcription. Also, a significant decrease in DNA methylation occurs. In addition, during the transcription stopping stage, H4 histone is methylated, forming large size H4K4m3, which plays an important role in activating the transcription of the zygote genome[4,21].

2.6. *mTOR* Signaling Pathway and Oocyte

The mammalian target of rapamycin (*mTOR*) is a serine/threonine-protein kinase that phosphorylates specific molecules to activate pathways that play a role in cell growth, cell division and many biological processes in response to growth factors, IGF-1, IGF-2 and nutrients such as amino acids. It is encoded by the *mTOR* gene and is contained in two different complexes, each consisting of an interconnected set of proteins and these two complexes are called Mammalian target of rapamycin complex 1 (mTORC1) and Mammalian target of rapamycin complex 2 (mTORC2). *mTORC1* consists of *mTOR*, Raptor, Deptor, mLST8 and PRAS40, and it can be regulated by rapamycin as rapamycin can inhibit it by binding to FK506-binding protein 12 (FKBp12) in the cells. mTORC2

consists of mTOR, Rictor, Deptor, mLST8, mSIN1 and Protor1/2, and it cannot be regulated by rapamycin[78]. mTORC1 is stimulated by signals from, glucose, insulin, cellular energy, cytokine, and oxygen, in addition to growth factors and amino acids, and it regulates anabolic processes such as protein synthesis, transcription, mitochondrial metabolism, lipid synthesis, ribosome biogenesis, aerobic glycolysis and nucleotide synthesis and catabolic processes such as autophagy, apoptosis, and mRNA degradation[79,80]. mTORC2 plays a role in the polymerization of actin and cytoskeletal control[81]. *mTOR* controls cell growth by producing proteins (mRNA translation), through modifications of phosphorylation and stimulation of transcription of ribosomal RNA, which stimulates ribosome biogenesis[78,82]. *mTOR* has been shown to play an important role in providing synaptic plasticity and in brain development and aging[79]. Also, dysfunction of *mTOR* leads to cancer, type 2 diabetes, obesity, neurodegenerative disorders and cardiovascular disease[22].

mTOR supports follicle development starting from stimulating primordial follicle growth and up to the formation of high-quality and haploid mature oocytes. It is involved in several biological processes that promote mitotic and cytoplasmic maturation and somatic cell differentiation and proliferation[25]. In the primordial follicle, the PI3K\AKT pathway contributes to the inhibition of the tumor suppressor complex (Tsc1/Tsc2), a negative regulator of mTORC1, which leads to mTORC1 activation[83]. mTORC1 phosphorylates 4E-BP1 and p70S6 kinase 1 (S6K1), which leads to stimulation of protein translation and follicle development (Figure 2.6)[23].

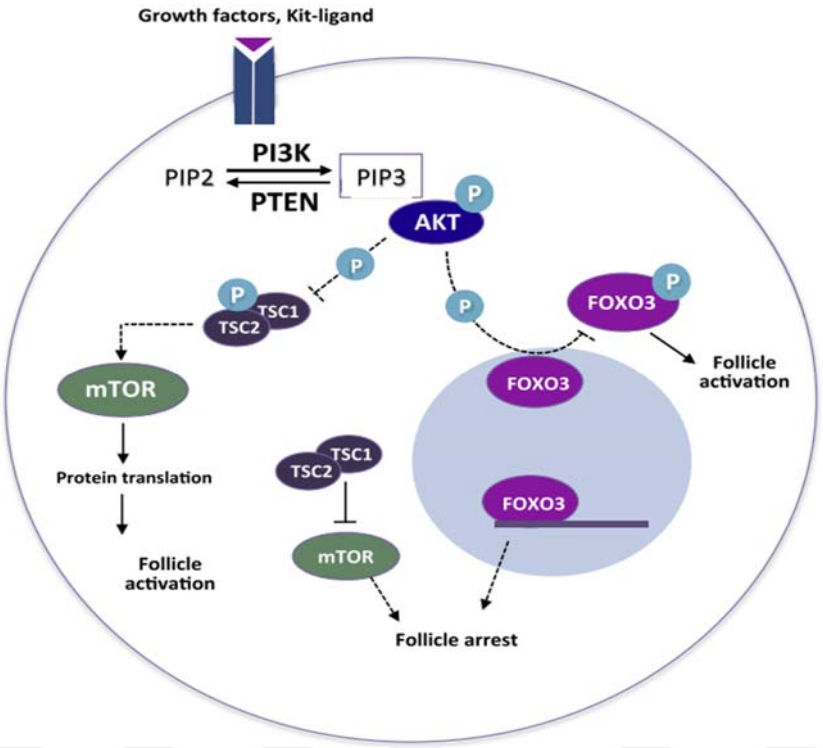

Figure 2.6. Schematic representation of the involvement of PI3K/PTEN and TSC/*mTOR* pathways in primordial follicle activation and arrest[23].

During meiotic maturation, mTORC1 localizes on the MS and condenses around chromosomes and regulates chromosomal alignment and its segregation, and mTORC2 condenses around MS and contributes to the assembly and polymerization of actin filaments[24]. *mTOR* also contributes to somatic cell proliferation as FSH activates *mTOR* in granulosa cells and LH activates *mTOR* in theca cells and this also supports steroidogenesis[24,84]. Inhibition of *mTOR* does not prevent follicle development but rather results in the maturation of defective follicles, deformed spindles, translation defects, asymmetric chromosomal segregation, DNA damage and immature somatic cells similar to Sertoli cells[22,85]. However, some studies have shown that inhibiting mTORC1 in pre-granulosa cells disrupts follicular activation while inhibiting it in oocytes does not affect follicle growth[86]. As for mTORC2 inhibition, it leads to the death of a large number of follicles. In vitro, it was observed that inhibition of *mTOR* by rapamycin prevented follicle growth and led to the appearance of oocyte-free follicles[28]. Overactivity of the *mTOR*

pathway leads to follicular overactivity and consequent follicular depletion and premature ovarian failure (POF)[26]. In short, *mTOR* plays an important role in maintaining the balance between primordial follicle activation and dormancy[27].

2.7. *c-Abl* Protein Tyrosine Kinase and Oocyte

c-Abl is a non-receptor tyrosine kinase encoded by the ABL-1[87]. It coordinates many biological functions to help cells differentiate, grow, divide, migrate, programmed death, morphogenesis, adhesion and many other processes[88,89]. It is stimulated by specific pathways activated by growth receptors, cytokines, and oxidative stress (RTKs) such as (EGF, PDGF, WEGE and ROS receptor families). When oxidative stress and DNA damage occur, its activity increases, inducing apoptosis[89,90]. c-Abl is constantly changing its position between the nucleus and the cytoplasm with the help of additional locational signals present in its C-terminal region: they are NLS (nuclear localization signals) and NES (nuclear export signal). NES transports c-Abl into the cytoplasm where it binds to F-actin and NLS transports *c-Abl* to the nucleus, where it binds to the DNA (Figure 2.7.a)[89].

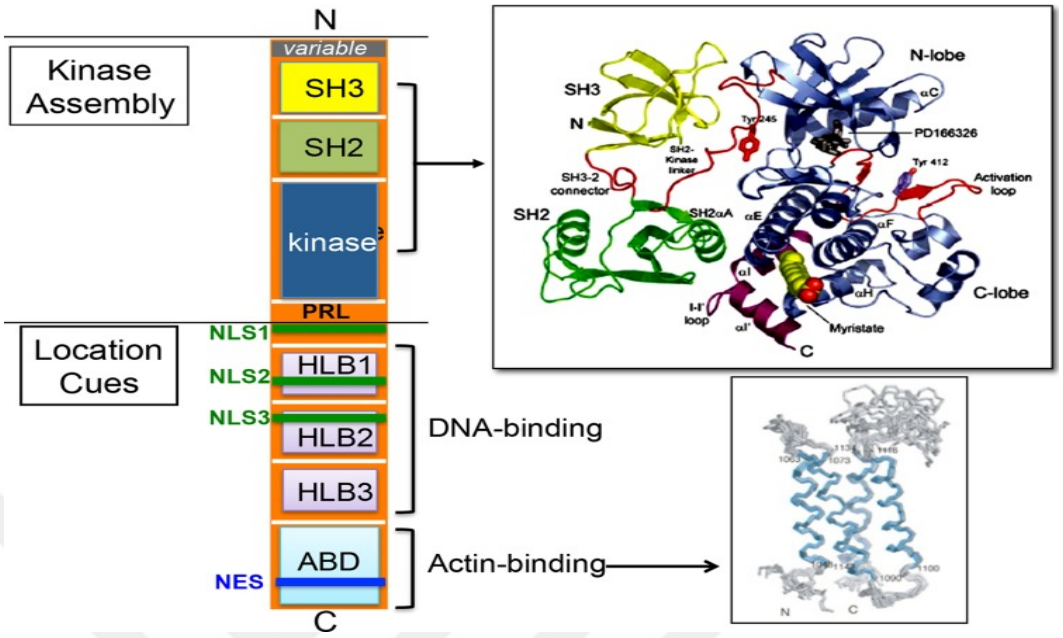

Figure 2.7.a. Schematic diagram of ABL domains and structures. N, N terminal; variable. SH3, Src homology 3 domain (yellow); SH2, Src homology 2 domain (green); kinase, kinase domain (blue). A proline-rich linker (PRL) binds to the kinase domain. NLS, nuclear localization signal; NES, nuclear export signal; HLB, HMG-like box; ABD, actin-binding domain[89].

c-Abl regulates the cytoskeleton of actin through phosphorylation of proteins involved in membrane anchoring, microtubule-binding and branch formation[91]. *c-Abl* plays a role in cell migration, endocytosis, stress response and synapse formation[89,92]. In the nucleus, *c-Abl* phosphorylates the C-terminal repeated domain (CTD) of RNA polymerase II, leading to activation of transcription and chromatin-modifying proteins[91,93]. The absence of *c-Abl* leads to DNA damage, impaired vascular function, insufficient muscle response, neurodegeneration, and fetal growth defects[89].

c-Abl is required to maintain genome integrity in oocytes as it repairs DNA double-strand breaks (DSBs) that naturally occur during meiosis and mitosis or when exposed to external factors such as radiation or endogenous factors such as oxidative stress. DNA damage induces *c-Abl* via ATM, DNA-PK and others[29]. *c-Abl* phosphorylates proteins responsible for DNA homologous recombination such as RAD51, RAD52, BRCA1, and MSH5, and can also repair the damage on its own by attaching its C-terminal segment directly to the cross-links within the DNA. When it is

unable to repair DNA damage, it stimulates apoptosis, this usually occurs on exposure to chemotherapy, as it phosphorylates TAP63 and P53, which are responsible for the death of the oocyte to prevent the formation of cancerous tumors (Figure 2.7.b)[29,94].

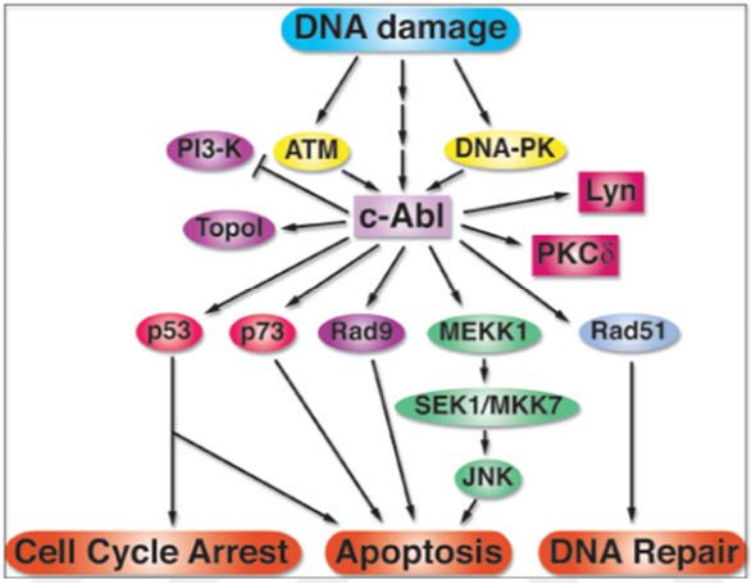

Figure 2.7.b. A role of *c-Abl* in response to DNA damage[94].

The absence of *c-Abl* results in the death of follicles or the development of defective oocytes[29]. In culture, imatinib, a *c-Abl* inhibitor, led to the death of follicles, while it had the opposite effect in cancer patients. DNA damage caused by a cancer treatment called cisplatin leads to the activation of *c-Abl*, which in turn leads to the apoptosis of follicles and depletion of the follicle reserve[31]. On exposure to ionizing radiation and other DNA damaging agents, c-Abl inhibits the telomerase enzyme by phosphorylation of the telomerase reverse transcriptase (TERT) catalyst unit, which leads to shortening of the telomeres, thus stimulating apoptosis, and thereby preventing the formation of tumors[95]. Also, one study showed that *c-Abl* controls telomere in granulosa cells by interaction with TERT, and that inhibition of *c-Abl* led to a reducing regulation of telomerase function and a gradual decrease in the proliferation of granulosa cells[32]. Imatinib led to apoptosis of granulosa cells[33]. Because it plays a role in regulating the cytoskeleton of F-actin, it supports meiotic maturation by regulating the mechanism of spindle action and correct separation of chromosomes[30].

2.8. Interaction Between *c-Abl* Tyrosine Kinase and *mTOR* Signaling Pathway

When DNA damage occurs, DNA damage sensors such as DNA-dependent protein kinase (DNA-PK) and ataxia–telangiectasia mutated (ATM) activate *c-Abl* that interacts with mouse double minute 2 homolog (MDM2) - a P53 inhibitor - so that P53 is released and accumulates in the cell (Figure 2.7.b)[34,35,96]. P53 activates 5'AMP-activated protein kinase (AMPK) via sestrin proteins. AMPK inhibits the anabolic processes in the cell and activates the TSC1 / TSC2 complex, which inhibits *mTOR*[97,98]. This leads to the de phosphorylation of S6K1 and the release of 4E-BP1, which forms a complex with the set of proteins required for cap-dependent translation, this leads to the stopping of mRNA translation and the degeneration of the proteasomes, thus arresting the cell cycle in G1 or undergoing the cell to apoptosis (Figure 2.8)[34,35].

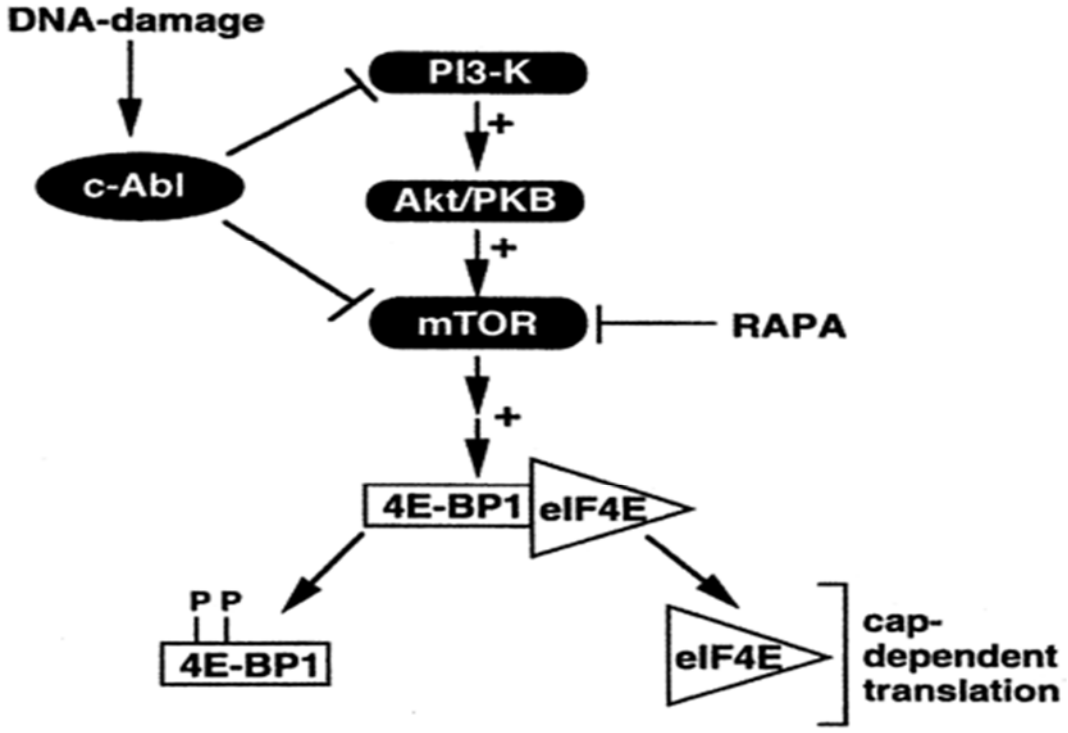

Figure 2.8. Schematic model of *c-Abl*-mediated regulation of the *mTOR*/RAFT1/FRAP cascade and 5 ′ cap-dependent translation[34].

Also, when DNA damage occurs, *c-Abl* inhibits AKT via phosphorylation of P38, thus inhibiting *mTOR*[34]. Inhibition of *mTOR* causes continuous activation of c-Jun N-

terminal kinases (JNK). This helps *c-Abl* cross over into the nucleus to repair DNA damage [99].

It is worth noting that the defects of oocyte maturation have been increasing in recent years. Studies have proven that this phenomenon is related to genetic defects and protein changes. We have previously shown that *mTOR* and *c-Abl* proteins play an important role in the meiotic and cytoplasmic maturation of oocytes. Therefore, in this study, we hypothesized that there is a very important association between *c-Abl* and *mTOR* during the process of oocyte maturation. To test our hypothesis, GV oocytes were cultured in a medium containing rapamycin (*mTOR* inhibitor) and imatinib (*c-Abl* inhibitor). The effect of these inhibitors on the rate of oocyte maturation and oocyte morphology was evaluated, after which the percentage of gene expression for *c-Abl* and *mTOR* was detected and the relationship between them was shown at the mRNA level.

3. MATERIALS AND METHODS

3.1. Oocyte Collection and Culture and Experimental Design:

18 female 6-8 week-old Balb/C mice were used in oocyte culture. Experiments were approved by the Animal Care and Use Committees of Yeditepe University (Protocol no: 2021-031). Superovulation was induced by intraperitoneal injections of 7,5 IU of pregnant mare's serum gonadotropin (Biovendor, 10.000 IU, #RP17827210000). After 46–48 h, mice were sacrificed via cervical dislocation and the ovaries were excised without oviducts or any fat and placed into a collection dish containing a HEPES-buffered medium. To obtain GV-staged oocytes from Graafian follicles, while observing with a stereomicroscope, the ovary was dissected with a syringe. Cumulus cells were removed by repeatedly pipetting. Using a mouth-operated glass pipette, GV-staged oocytes were collected and randomly divided into the drops of KSOM (Sigma, #MR-106-D) medium covered with mineral oil and cultured in an incubator (5% CO_2 at 37°C) after being imaged via the ZEISS Axio Observer microscope.

We designed 3 main groups as GV, MI and MII stage oocytes. Additionally, we used 2 different treatment groups as imatinib (inhibitor of *c-Abl*, 1 µM, 5 µM and 10 µM) and rapamycin (inhibitor of *mTOR*, 1000 µM). All the experimental groups are shown in table 3.1.

Table 3.1. Experimental design of the study.

	GV Oocyte	MI Oocyte	MII Oocyte
1µM Imatinib			
5µM Imatinib			
10µM Imatinib			
1000µM Rapamycin			
Control			
DMSO			

Imatinib Mesylate (CGP-57148B, STI-571, BioVision, #1625) was prepared by dissolving in DMSO (Sigma, #D8418) for stock concentration. Concentrations were prepared by diluting in KSOM (Sigma, #MR-106-D) (1 μM, 5 μM, 10 μM). Imatinib (STI57) doses required to inhibit endogenous Abl kinases were not available in the literature, so studies with somatic cells in the literature were used[100-102]. Rapamycin (Glentham Life Science, #GA7417) was prepared by dissolving in DMSO (Sigma, #D8418). Concentrations were prepared by diluting in KSOM (Sigma, #MR-106-D) (1000 μM). For the DMSO group, only the same amount of solvent DMSO (Sigma, #D8418) was used. For the control group, only KSOM (Sigma, #MR-106-D) was used.

GV-staged oocytes were cultured in these groups under mineral oil in the incubator (5% CO_2 at 37°C). The rate of GV, MI and MII were recorded after 16 h of culture and imaged via the Axio ZEISS Observer microscope.

Oocytes were denuded of their cumulus cells by exposure to hyaluronidase or mechanical method using pipettes and then washed with PBS. After that, from each group, GV, MI, and MII oocytes were separated into 3 tubes containing (20 μl) RNA lysis buffer and placed in a refrigerator at –20° C.

3.2. Oocyte Scoring

GV, MI and MII oocytes were evaluated based on 6 parameters: (i) Oocyte shape; (ii) oocyte size; (iii) ooplasm characteristics; (iv) zona pellucida (ZP); (v) structure of the perivitelline space (PVS); and (vi) polar body (PB) morphology. Each parameter was graded as worst (-1), average (0), or best (1), creating a total oocyte scoring (TOS) by adding up individual parameter assessments. The maximal TOS of MII oocyte, therefore, could be a +6, the lowest a -6. But, the maximal TOS of MI oocyte could be a +5, the lowest a -5 (Because it does not have a PB) and the maximal TOS of GV oocyte could be a +4, the lowest a -4 (Because it does not have a PB and PVS). The 6 individual parameters were assessed as shown in table 3.2[103].

Table 3.2. Oocyte scoring system[103].

	-1	0	+1
(i) Oocyte shape	Dark general oocyte coloration and/or ovoid shape	Less dark general oocyte coloration and less ovoid shape	Normal
(ii) Oocyte size	Abnormally small or large	For GV, MI and MII: did not deviate from normal by more than 10µm	For GV > 75µm and < 85µm [104,105] For MI: > 90µm and < 100µm For MII: > 100µm and < 110µm [106]
(iii) Ooplasm characteristics	Very granular and/or very vacuolated and/or several inclusions	Slightly granular and/or only a few inclusions	Absence of granularity and inclusions
(iv) Zona pellucida morphology	Very thin or thick	For GV, MI, and MII: did not deviate from normal by more than 2µm	For GV, MI and MII: > 7µm and < 8µm [107,108]
(v) Structure of the perivitelline space	Abnormally large PVS, an absent PVS, or a very granular PVS	Moderately enlarged PVS and/or small PVS and/or a less granular PVS	Normal size PVS with no granules
(vi) Polar body morphology	Flat and/or multiple PBs, granular and/or either abnormally small or large PBs	Fair but not excellent	Normal size and shape

Not: We have considered that the ideal size of an MI oocyte is between 90 and 100 µm, as its size is close to the size of the MII oocyte.

Measurements were taken and properties were evaluated from images captured by the Axio ZEISS Observer microscope using ZEN imaging software (Figure 3.2)

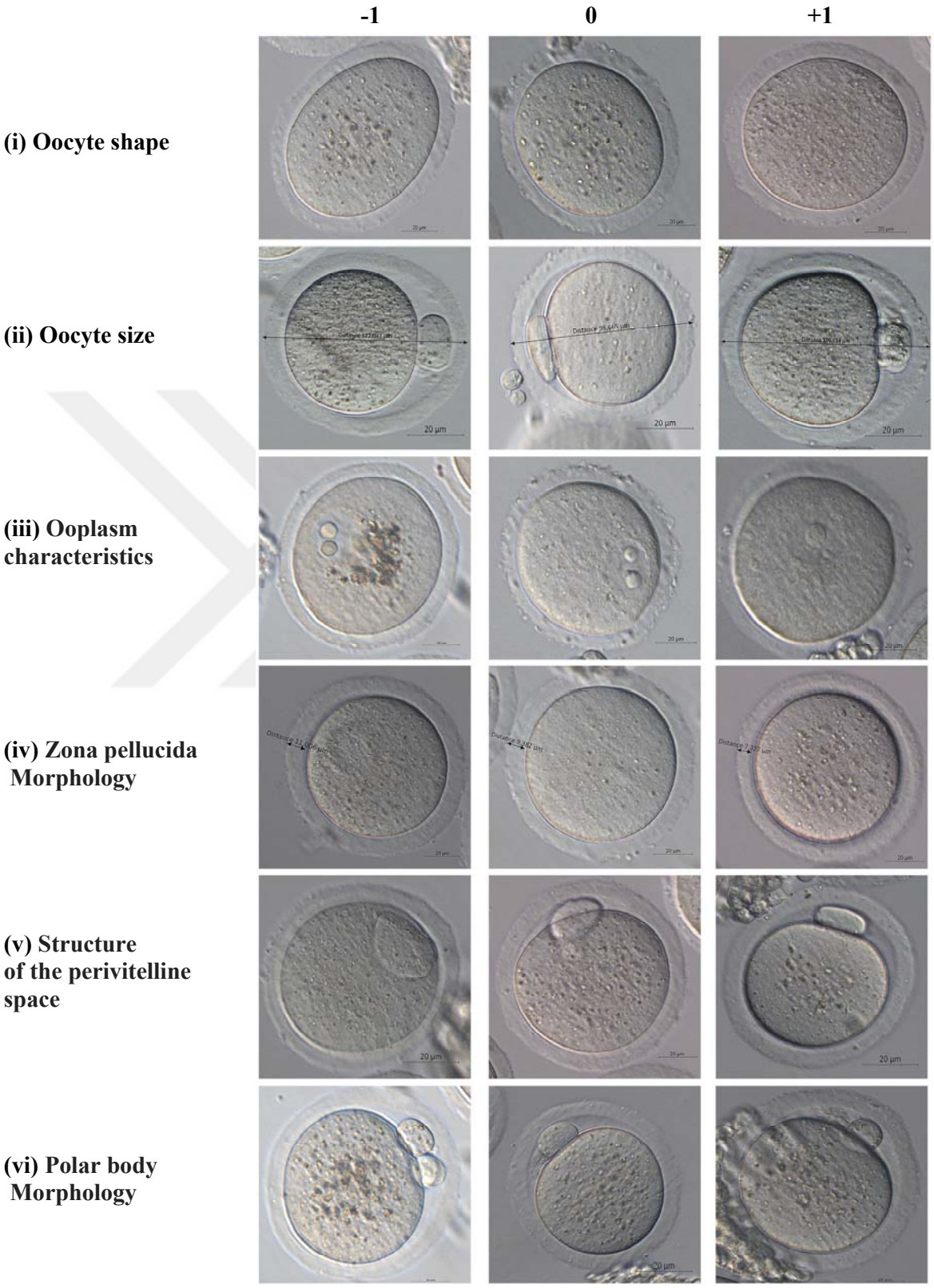

Figure 3.2. Example photographs for oocyte scoring system.

3.3. qRT-PCR

The *c-Abl* and mTOR mRNA levels were detected by quantitative RT-PCR. *c-Abl* and *mTOR* mRNA expressions were detected at the GV, MI and MII stages.

3.3.1. RNA Isolation

Total RNA was extracted from each group by using the Total RNA Purification Kit- Column Kit (Jena Bioscience, #PP210S).

RNA samples were taken in 20 µl Lysis Buffer. Then, the 2-Propanol was added to the RNA samples to be 0.6 times the lysis solution in which it is present and pipetting was done. Filter column and 2 ml microcentrifuge tubes were prepared, then 100 µl activation buffer was added to the filters. They were centrifuged for 30 seconds at 10,000 g and then the flow-through was discarded. Samples on which 2-propanol was added were transferred to the column. They were centrifuged for 30 seconds at 10,000 g and then the flow-through was discarded. After that, 700 µl first washing buffer was added to the columns. It is centrifuged for 30 seconds at 10,000 g and then the flow-through was discarded. Then, 700 µl second washing buffer was added to the columns. They were centrifuged for 30 seconds at 10,000 g and then the flow-through was discarded. After the microcentrifuge tube has been emptied, the empty tube and the column were centrifuged again at 10,000 g for 2 min (to remove any remaining alcohol in the filter). The columns were transferred to DNase/RNase-free microcentrifuge tubes and 40 µl of elution buffer was added. Then they were incubated for 1 min at room temperature and centrifuged for 1 minute at 10,000 g. The obtained RNA was stored at -20^{o}C. RNA quality and concentration were determined using a NanoDrop 2000 spectrophotometer (Thermo Scientific) (Table 3.3.1).

Table 3.3.1. RNA concentration in experimental groups.

Groups	Oocyte Stage	RNA concentration
Control	GV	12.6 ng/ml
	MI	11.8 ng/ml
	MII	10.7 ng/ml
DMSO	GV	13.4 ng/ml
	MI	13.0 ng/ml
	MII	12.6 ng/ml
1 µM imatinib	GV	7.4 ng/ml
	MI	9.6 ng/ml
	MII	8.1 ng/ml
5 µM imatinib	GV	8.4 ng/ml
	MI	9.3 ng/ml
	MII	7.0 ng/ml
10 µM imatinib	GV	11.0 ng/ml
	MI	9.3 ng/ml
	MII	10.7 ng/ml
1000 µM rapamycin	GV	15.4 ng/ml
	MI	14.5 ng/ml
	MII	12.0 ng/ml

To prepare buffers:

Lysis Buffer: Before using the lysis buffer, 260 µl of 2-mercaptoethanol is added to 26 ml of lysis buffer.

First Washing Buffer: 8 ml of 100% ethanol is added to 32 ml of the first washing buffer. Second Washing Buffer: 32 ml of 100% ethanol is added to 8 ml of second washing Buffer.

3.3.2. cDNA Synthesis

Total RNA was used to reverse cDNA with SCRIPT cDNA Synthesis Kit, (Jena Bioscience, #PCR511S). The master mix was prepared as shown in table 3.3.2. PCR tubes were prepared for each sample with 9.5 µl of RNA and 0.5 µl of oligo-dT, mixed and

incubated at 75 ºC for 5 minutes. Then, 10 µl of the master mix was added to each reaction, incubated for 10 min at 42 ºC, then 60 min at 50 ºC.

Table 3.3.2. Preparation of the master mix.

SCRIPT RT Buffer	4 µl
dNTP Mix	1 µl
DTT Stock Solution	1 µl
RNase inhibitor	1 µl
SCRIPT Reverse Transcriptase	0.5 µl
RNase-free Water	2.5 µl
	10 µl mix

3.3.3. qReal Time PCR

SYBR Green qPCR was used to detect the expression of c-*Abl* and *mTOR*. cDNA was assayed in triplicate. Each 12 µl reaction contained 9 µl of 2x Maxima SYBR Green qPCR Master Mix, 1 µl (1 nM) of forward primer, 1 µl (1 nM) of reverse primer and 1 µl Template DNA. *β-Actin* was chosen as the reference gene. The sequences of the primers used are presented in table 3.3.3. Quantitative RT-PCRs carried out on a CFX96 Touch™ Real-Time PCR Detection System (Bio-Rad Laboratories), in which the initial 3 min for denaturation at 95°C followed by 55 cycles of 95°C/15 sec, 47°C/30 sec and 55°C/30 sec for *c-Abl* and 5 min for denaturation at 94°C following by 35 cycles of 94°C/30 sec, 59°C/1 min and 72°C/45 sec for *mTOR*. All expression data were normalized by dividing the amount of the target gene by the amount of *β-actin*.

Table 3.3.3. The sequences of the primers.

c-Abl	F- CGG GAC CAT GTT GGA GAT R- TTC ATA CCG CAG CGA GATG
mTOR	F- TTGGAGTGGCTGGGTGCTGA R- AAGGGCTGAACTTGCTGGAA
β-Actin	F- GAT GAC GAT ATC GCT GCG CTG R- GTA CGA CCA GAG GCA TAC AGG

3.4. STATISTICAL ANALYSIS

At least three biological replicates were used for each analysis. Each replicate was done by an independent experiment at a different time. Results are given as means ± SEM. Statistical comparisons were made using analysis of One-way ANOVA. To evaluate *c-Abl* and *mTOR* together, Two-way ANOVA was used. *P*-value < 0.1 was considered statistically significant. In all figures, one (1), two (2), three (3), and four (4) asterisks indicate *$p < 0.1$, **$p < 0.01$, ***$p < 0.001$, and ****p<0.0001, respectively.

4. RESULTS

4.1. Rate of oocyte maturation

To examine the functional roles of *mTOR* and *c-Abl* during oocyte maturation, we treated germinal vesicle (GV) oocytes with 2 different treatment groups as imatinib (1 µM, 5 µM and 10 µM) and rapamycin (1000 µM). Then, the developmental potential of GV oocytes to the MII stage was evaluated and the rate of GV, MI and MII were recorded after the culture period. All the experiments were repeated for 4 times.

Experiment 1: 135 GV-staged oocytes were obtained from the mouse ovary. The rate of GV, MI and MII were recorded after 16 h of culture (Table 4.1.1).

Table 4.1.1. Rate of oocyte maturation in experiment 1 after 16 h of culture.

	Total Isolated GV Oocyte	**GV Arrest**	**MI Arrest**	**MII**	**GV% Arrest**	**MI% Arrest**	**MII%**
1 µM imatinib	21	6	7	8	28.6%	33.3%	38.1%
5 µM imatinib	19	2	9	8	10.5%	47.4%	42.1%
10 µM imatinib	20	4	14	2	20%	70%	10%
1000 µM rapamycin	17	0	12	5	0%	70.6%	29.4%
Control	16	1	9	6	6.25%	56.25%	37.5%
DMSO	21	3	10	8	14.3%	47.6%	38.1%

Experiment 2: 100 GV-staged oocytes were obtained from the mouse ovary. The rate of GV, MI and MII were recorded after 16 h of culture (Table 4.1.2).

Table 4.1.2. Rate of oocyte maturation in experiment 2 after 16 h of culture.

	Total Isolated GV Oocyte	**GV Arrest**	**MI Arrest**	**MII**	**GV% Arrest**	**MI% Arrest**	**MII%**
1 µM imatinib	17	2	11	4	11.8%	64.7%	23.5%
5 µM imatinib	14	5	6	3	35.7%	42.9%	21.4%
10 µM imatinib	12	1	10	1	8.33%	83.33%	8.33%
1000 µM rapamycin	13	2	4	7	15.4%	30.8%	53.8%
Control	13	3	3	7	23.1%	23.1%	53.8%
DMSO	12	1	5	6	8.3%	41.7%	50%

Experiment 3: 99 GV-staged oocytes were obtained from the mouse ovary. The rate of GV, MI and MII were recorded after 16 h of culture (Table 4.1.3).

Table 4.1.3. Rate of oocyte maturation in experiment 3 after 16 h of culture.

	Total Isolated GV Oocyte	**GV Arrest**	**MI Arrest**	**MII**	**GV% Arrest**	**MI% Arrest**	**MII%**
1 µM imatinib	17	3	8	6	17.7%	47.1%	35.3%
5 µM imatinib	20	8	2	10	40%	10%	50%
10 µM imatinib	16	0	14	2	0%	87.5%	12.5%
1000 µM rapamycin	15	1	6	8	6.7%	40%	53.4%
Control	21	1	14	6	4.8%	66.7%	28.6%
DMSO	11	2	7	2	18.2%	63.6%	18.2%

Experiment 4: 72 GV-staged oocytes were obtained from the mouse ovary. The rate of GV, MI and MII were recorded after 16 h of culture (Table 4.1.4).

Table 4.1.4. Rate of oocyte maturation in experiment 4 after 16 h of culture.

	Total Isolated GV Oocyte	**GV Arrest**	**MI Arrest**	**MII**	**GV% Arrest**	**MI% Arrest**	**MII%**
1 µM imatinib	13	2	5	6	15.4%	38.5%	46.1%
5 µM imatinib	11	2	8	1	18.8%	72.7%	9.1%
10 µM imatinib	14	2	9	3	14.3%	64.3%	21.4%
1000 µM rapamycin	7	3	3	1	42.85%	42.85%	14.3%
Control	14	2	6	6	14.3%	42.85%	42.85%
DMSO	8	1	3	4	12.5%	37.5%	50%

Then, the total rate of oocyte maturation in all experiments after 16 h of culture was recorded as shown in the table (Table 4.1.5).

Table 4.1.5. Total rate of oocyte maturation in all experiments after 16 h of culture.

	Total Isolated GV Oocyte	**GV Arrest**	**MI Arrest**	**MII**	**GV% Arrest**	**MI% Arrest**	**MII%**
1 µM imatinib	68	13	31	24	19.1%	45.6%	35.3%
5 µM imatinib	64	17	25	22	26.6%	39%	34.4%
10 µM imatinib	62	7	47	8	11.3%	75.8%	12.9%
1000 µM rapamycin	52	6	25	21	11.5%	48.1%	40.4%
Control	64	7	32	25	11%	50%	39%
DMSO	52	7	25	20	13.5%	48.1%	38.5%

In the rapamycin group, we observed that the percentage of GV oocytes did not differ significantly from that in the control and DMSO groups (11.5%, 11%, and 13.5%, respectively). We also observed that the percentage of MI oocytes that could develop from GV to MI did not differ significantly compared to that in the control and DMSO groups (48.1%, 50% and 48.1%, respectively). We also observed that the percentage of MII oocytes that could develop from MI to MII slightly increased compared to that in the control and DMSO groups (40.4%, 39% and 38.5%, respectively).

In the 1 µM imatinib group, we observed that the percentage of GV oocytes slightly increased compared to that in the control and DMSO groups (19.1%, 11% and 13.5%). We also observed that the percentage of MI oocytes slightly decreased compared to that in the control and DMSO groups (45.6%, 50% and 48.1%). We also observed that the percentage of MII oocytes slightly decreased compared to that in the control and DMSO groups (35.3%, 39% and 38.5%).

In the 5 µM imatinib group, we observed that the percentage of GV oocytes increased compared to that in the control and DMSO groups (26.6%, 11% and 13.5%). We also observed that the percentage of MI oocytes decreased compared to that in the

control and DMSO groups (39%, 50% and 48.1%). We also observed that the percentage of MII oocytes decreased compared to that in the control and DMSO groups (34.4%, 39% and 38.5%).

In the 10 μM imatinib group, we observed that the percentage of GV oocytes did not differ significantly from that in the control and DMSO groups (11.3%, 11% and 13.5%). We also observed that the percentage of MI oocytes greatly increased compared to that in the control and DMSO groups (75.8%, 50% and 48.1%). We also observed that the percentage of MII oocytes greatly decreased compared to that in the control and DMSO groups (12.9%, 39% and 38.5%).

4.2. Oocyte Scoring Results

In order to detect the effect of *mTOR* and *c-Abl* on oocyte morphology during oocyte maturation, GV, MI and MII oocytes were evaluated based on 6 parameters as shown in table 3.2. The maximal TOS of MII oocyte is +6, the lowest -6. The maximal TOS of MI oocyte is +5, the lowest -5 and the maximal TOS of GV oocyte is +4, the lowest -4.

Experiment 1: The oocytes were gathered according to their total score (Table 4.2.1).

Table 4.2.1. Total oocyte scoring in experiment 1.

	GV									**MI**											**MII**											
	-4	**-3**	**-2**	**-1**	**0**	**+1**	**+2**	**+3**	**+4**	**-5**	**-4**	**-3**	**-2**	**-1**	**0**	**+1**	**+2**	**+3**	**+4**	**+5**	**-6**	**-5**	**-4**	**-3**	**-2**	**-1**	**0**	**+1**	**+2**	**+3**	**+4**	**+5**	**+6**
1 µM imatinib							2	2	1								1	4	1								1	2	4	1			
5 µM imatinib							2	1								2	1	3	3							3	2	2		1			
10 µM imatinib							2	2					1	2	4	2	2	3										1	1				
1000 µM rapamycin																1	3	2	2						1		1	1	2	1			
Control							1									1	2	3	2					1		1	1	2	1	1			
DMSO							1	1	1							1		3	5					1				4	2	1			

Experiment 2: The oocytes were gathered according to their total score (Table 4.2.2).

Table 4.2.2. Total oocyte scoring in experiment 2.

	GV					MI										MII											
	-	-	-	-	0	+	+	+	+	-	-	-	-	-	0	+	+	+	+	-	-	-	-	-	0	+	+	+	+	+
	4	3	2	1		1	2	3	4	5	4	3	2	1		1	2	3	4	5	5	4	3	2	1	1	2	3	4	5	6
1 µM imatinib						2								1		3	4	2	1				1		1	1					
5 µM imatinib					1	2	2	2	1					1	1	1	1	1							2	1					
10 µM imatinib						2									1	3	4	2								1					
1000 µM rapamycin						1		1	1							1	1	1							1	1	2	1			
Control							1	1	1							1	2									4	2	1			
DMSO						1										1	2								1	1	2	1			

Experiment 3: The oocytes were gathered according to their total score (Table 4.2.3).

Table 4.2.3. Total oocyte scoring in experiment 3.

	GV					MI						MII											
	- 4	- 3	- 2	- 1	0	+ 1	+ 2	+ 3	+ 4	- 5	- 4	- 3	- 2	- 1	0	+ 1	+ 2	+ 3	+ 4	- 6	- 5	- 4	- 3	- 2	1	+ 1	+ 2	+ 3	+ 4	+ 5	+ 6
1 µM imatinib						2		1						1									1			1	3	1				
5 µM imatinib			1		1	4	1	1										1	1					1	2	3	3				
10 µM imatinib						2							1	2	1			3	1	1				1	1	1						
1000 µM rapamycin						1									1			3	2							1	1	4	2			
Control						1								1	1		1	2	2	6							3	2	1			
DMSO								1					1	1			1	1	1	2						1			1			

Experiment 4: The oocytes were gathered according to their total score (Table 4.2.4).

Table 4.2.4. Total oocyte scoring in experiment 4.

	GV					MI										MII											
	-	-	-	-	0	+	+	+	+	-	-	-	-	-	+	+	+	+	+	+	-	-	-	-	-	+	+	+	+	+	+
	4	3	2	1		1	2	3	4	5	4	3	2	1	0	1	2	3	4	5	6	5	4	3	2	1	0	1	2	3	4	5	6
1 µM imatinib					1	1									4	1	1								1	1	1		1		1		
5 µM imatinib						1	1				1		1	1	1	1									1			1					
10 µM imatinib			1	1	0							1	1	4	1									1			0					
1000 µM rapamycin					1	1	1								1	1		1								1							
Control						1	1								1		2	3									1	2	2	1			
DMSO						1					1	1				1											1	2	2				

For all experiments, the oocytes were gathered according to their total score (Table 4.2.5).

Table 4.2.5. Total oocyte scoring in all experiment.

	GV								MI										MII											
	-	-	-	-	0	+	+	+	+	+	-	-	-	-	-	0	+	+	+	+	+	+	-	-	-	-	-	-	+	+	+
	4	3	2	1		1	2	3	4	5	4	3	2	1		1	2	3	4	5	6	5	4	3	2	1		1	2	3	4	5	6
1 µM imatinib					1	3	4	3	1					2		10	8	10	2						2	1	2	4	6	6	1	1		
5 µM imatinib				1		2	7	6	4	1			1	2	1	4	4	5	4							2	5	7	7			1		
10 µM imatinib			1	1	1	2	4	2				1	3	8	7	5	9	6	1						2	1	3	2	1				
1000 µM rapamycin					1	2	2	1	1						2	3	4	7	4						1	2	3	2	7	5			
Control						2	3	1	1						2	2	8	8	8					1		1	2	11	7	4			
DMSO						1	2	1	2		1	1	1		1	1	3	5	9					1		1	3	8	7	3			

Then, the oocytes were classified as worst (-1), average (0), or best (1) (Table 4.2.6).

Table 4.2.6. Classification of oocytes as worst (-1), average (0), or best (1).

	GV			MI			MII		
	-1	**0**	**+1**	**-1**	**0**	**+1**	**-1**	**0**	**+1**
1 µM imatinib		1	11	2		30	5	4	14
5 µM imatinib	1	2	18	4	1	17	9	7	8
10 µM imatinib	2	1	8	12	7	21	3	3	3
1000 µM rapamycin		1	6		2	18	3	3	14
Control DMSO			7		2	26	2	2	22
			6	3	1	18	2	3	18

Finally, the rate of worst (-1), average (0), and best (1) oocytes were calculated (Table 4.2.7).

Table 4.2.7. Rate of worst (-1), average (0) and best (1) oocytes.

	GV			MI			MII		
	-1	**0**	**+1**	**-1**	**0**	**+1**	**-1**	**0**	**+1**
1 µM imatinib	0%	8.3%	91.7%	6.25%	0%	93.75%	21.7%	17.4%	60.9%
5 µM imatinib	4.8%	9.5%	85.7%	18.2%	4.5%	77.3%	37.5%	29.2%	33.3%
10 µM imatinib	18.2%	9.1%	72.7%	30%	17.5%	52.5%	33.33%	33.33%	33.33%
1000 µM rapamycin	0%	14.3%	85.7%	0%	10%	90%	15%	15%	70%
Control	0%	0%	100%	0%	7.2%	92.8%	7.7%	7.7%	84.6%
DMSO	0%	0%	100%	13.6%	4.6%	81.8%	8.7%	13%	78.3%

In the rapamycin group, there was no difference in the percentage of bad GV oocytes compared to the control group and DMSO group (0%, 0% and 0%). The percentage of middle GV oocytes slightly increased compared to the control group and the DMSO group (14.3%, 0% and 0%). The percentage of good GV oocytes slightly decreased compared to the control group and the DMSO group (85.7%, 100% and 100%). There was no difference in the percentage of bad MI oocytes compared to the control group (0%, 0%), while the percentage slightly decreased compared to the DMSO group (0%, 13.6%). The percentage of middle MI oocytes slightly increased compared to the control group and the DMSO group (10%, 7.2% and 4.6%). The percentage of good MI oocytes slightly decreased compared to the control group (90%, 92.8%) and slightly increased compared to the DMSO group (92.8% and 81.8%). The percentage of bad MII oocytes slightly increased compared to the control group and the DMSO group (15%, 7.7% and 8.7%). The percentage of middle MII oocytes slightly increased compared to the control group and the DMSO group (15%, 7.7% and 13%). The percentage of good MII oocytes slightly decreased compared to the control group and the DMSO group (70%, 84.6% and 78.3%). In short, rapamycin has a slightly negative effect on the morphology of GV, MI and MII oocytes.

In the 1 μM imatinib group, there was no difference in the percentage of bad GV oocytes compared to the control group and DMSO group (0%, 0% and 0%). The percentage of middle GV oocytes slightly increased compared to the control group and the DMSO group (8.3%, 0% and 0%). The percentage of good GV oocytes slightly decreased compared to the control group and the DMSO group (91.7%, 100% and 100%). The percentage of bad MI oocytes slightly increased compared to the control group (6.25%, 0%) and slightly decreased compared to the DMSO group (6.25%, 13.6%). The percentage of middle MI oocytes slightly decreased compared to the control group and the DMSO group (0%, 7.2% and 4.6%). The percentage of good MI oocytes slightly increased compared to the control group and the DMSO group (93.75%, 92.8% and 81.8%). The percentage of bad MII oocytes slightly increased compared to the control group and the DMSO group (21.7%, 7.7% and 8.7%). The percentage of middle MII oocytes slightly increased compared to the control group and the DMSO group (17.4%, 7.7% and 13%). The percentage of good MII oocytes decreased compared to the control group and the DMSO group (60.9%, 84.6% and 78.3%). In short, 1 μM imatinib has a slightly negative effect on the morphology of GV, a negative effect on the morphology of MII oocytes and no negative effect on the morphology of MI oocytes.

In the 5 μM imatinib group, The percentage of bad GV oocytes slightly increased compared to the control group and the DMSO group (4.8%, 0% and 0%). The percentage of middle GV oocytes slightly increased compared to the control group and the DMSO group (9.5%, 0% and 0%). The percentage of good GV oocytes slightly decreased compared to the control group and the DMSO group (85.7%, 100% and 100%). The percentage of bad MI oocytes slightly increased compared to the control group and the DMSO group (18.2%, 0% and 13%). The percentage of middle MI oocytes slightly decreased compared to the control group and the DMSO group (4.5%, 7.2% and 4.6%). The percentage of good MI oocytes slightly decreased compared to the control group and the DMSO group (77.3%, 92.8% and 81.8%). The percentage of bad MII oocytes greatly increased compared to the control group and the DMSO group (37.5%, 7.7% and 8.7%). The percentage of middle MII oocytes increased compared to the control group and the DMSO group (29.2%, 7.7% and 13%). The percentage of good MII oocytes greatly decreased compared to the control group and the DMSO group (33.3%, 84.6% and 78.3%). In short, 5 μM imatinib has a slightly negative effect on the morphology of GV and MI and a negative effect on the morphology of MII oocytes.

In the 10 μM imatinib group, The percentage of bad GV oocytes increased compared to the control group and the DMSO group (18.2%, 0% and 0%). The percentage of middle GV oocytes slightly increased compared to the control group and the DMSO group (9.1%, 0% and 0%). The percentage of good GV oocytes greatly decreased compared to the control group and the DMSO group (72.7%, 100% and 100%). The percentage of bad MI oocytes increased compared to the control group and the DMSO group (30%, 0% and 13%). The percentage of middle MI oocytes slightly increased compared to the control group and the DMSO group (17.5%, 7.2% and 4.6%). The percentage of good MI oocytes greatly decreased compared to the control group and the DMSO group (52.5%, 92.8% and 81.8%). The percentage of bad MII oocytes greatly increased compared to the control group and the DMSO group (33.33%, 7.7% and 8.7%). The percentage of middle MII oocytes increased compared to the control group and the DMSO group (33.33%, 7.7% and 13%). The percentage of good MII oocytes greatly decreased compared to the control group and the DMSO group (33.3%, 84.6% and 78.3%). In short, 10 μM imatinib has a greatly negative effect on the morphology of GV, MI and MII oocytes.

We showed example photographs of oocytes scored after 0 h and 16 h for each group (Figure 4.2).

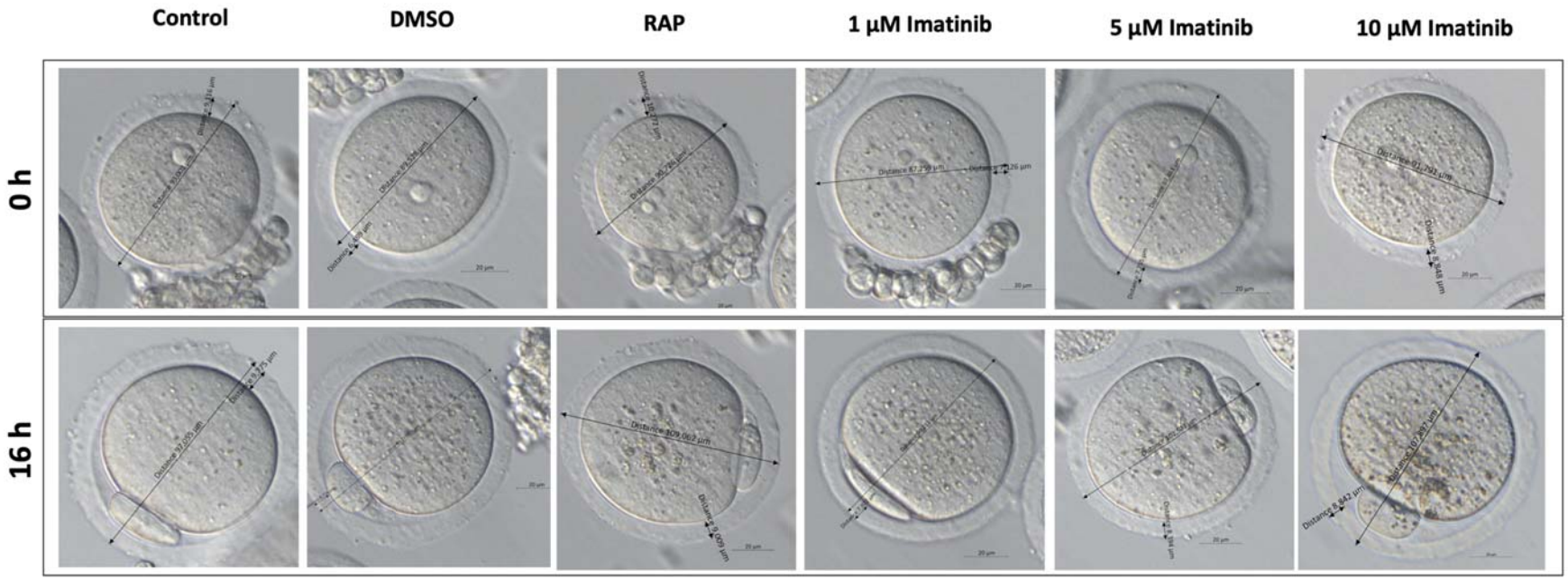

Figure 4.2. Example photographs of oocytes scored after 0 h and 16 h.

4.3. qRT-PCR Results

At the end of the 16 h incubation period, qRT-PCR was performed by grouping the oocytes at the GV, and MI stages which could not complete their maturation and the MII stage oocyte, *c-Abl* and *mTOR* expression were analyzed at mRNA level for each experimental group.

qRT-PCR results show the mRNA expression level of *mTOR* in mouse GV oocytes in all the experimental groups. Compared with the control group, *mTOR* expression level was significantly decreased in the 1 μM imatinib treatment group (*p<0.1) (Figure 4.3.1).

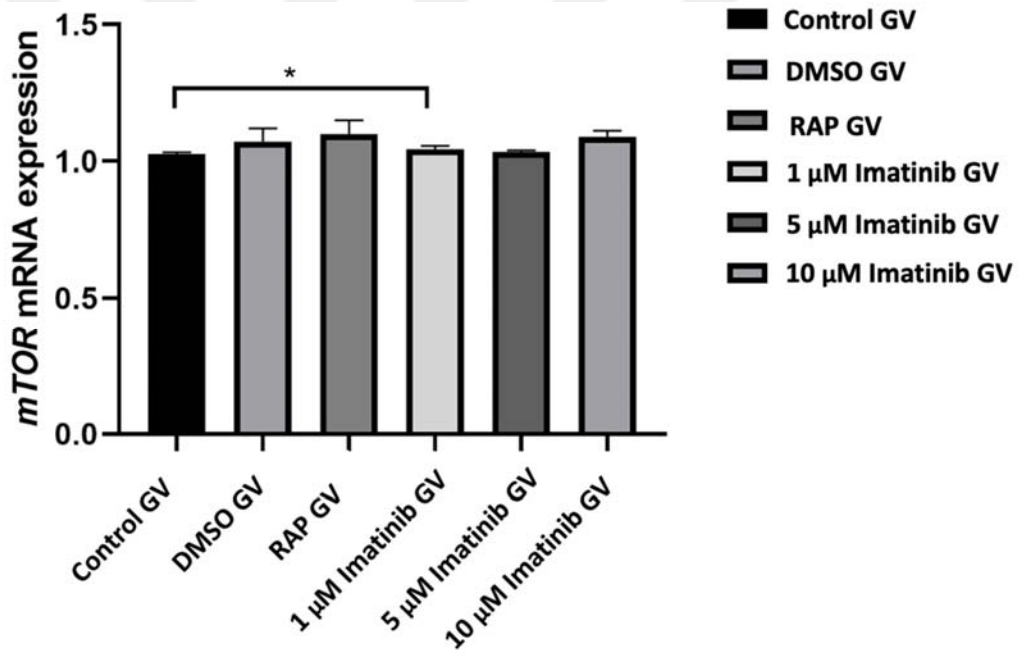

Figure 4.3.1. *mTOR* expression level in control, DMSO, 1000 μM rapamycin, 1 μM imatinib, 5 μM imatinib and 10 μM imatinib treatment at GV oocyte. Error bars indicate the SEM. n=3. (*p<0.1).

qRT-PCR results show the mRNA expression level of *mTOR* in mouse MI oocytes in all the experimental groups. Its expression was significantly increased in the 1000 μM rapamycin treatment group and expression was decreased in the 1 μM Imatinib treatment group (*p<0.1, **p<0.01) (Figure 4.3.2).

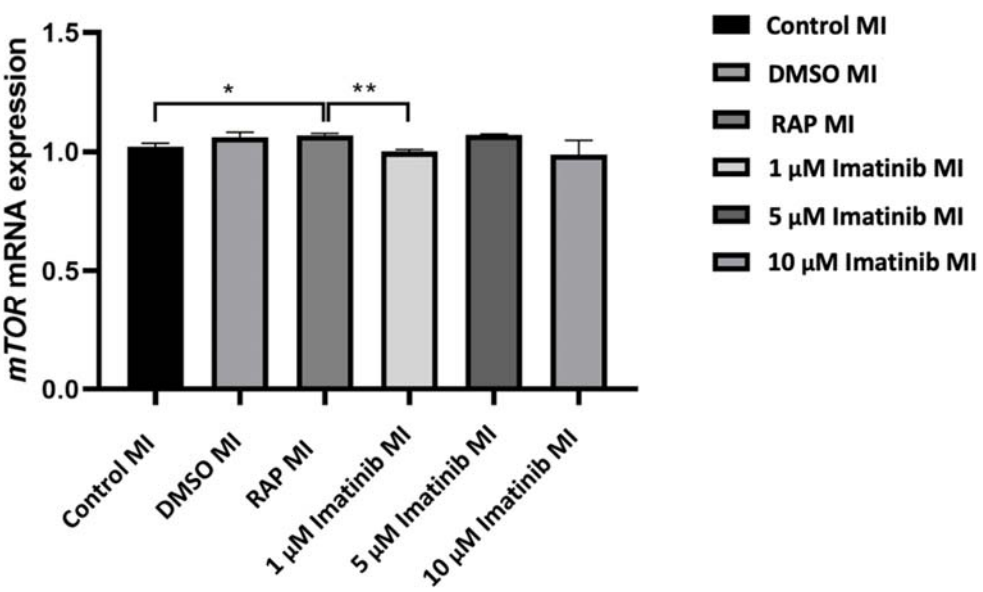

Figure 4.3.2. *mTOR* expression level in control, DMSO, 1000 μM rapamycin, 1 μM imatinib, 5 μM imatinib and 10 μM imatinib treatment at MI stage mouse oocyte. Error bars indicate the SEM. n=3. (*p<0.1, **p<0.01).

qRT-PCR results show the mRNA expression level of *mTOR* in mouse MII oocytes in all the experimental groups. mTOR expression level was significantly decreased in 1 μM and 10 μM imatinib groups (*p<0.1) (Figure 4.3.3).

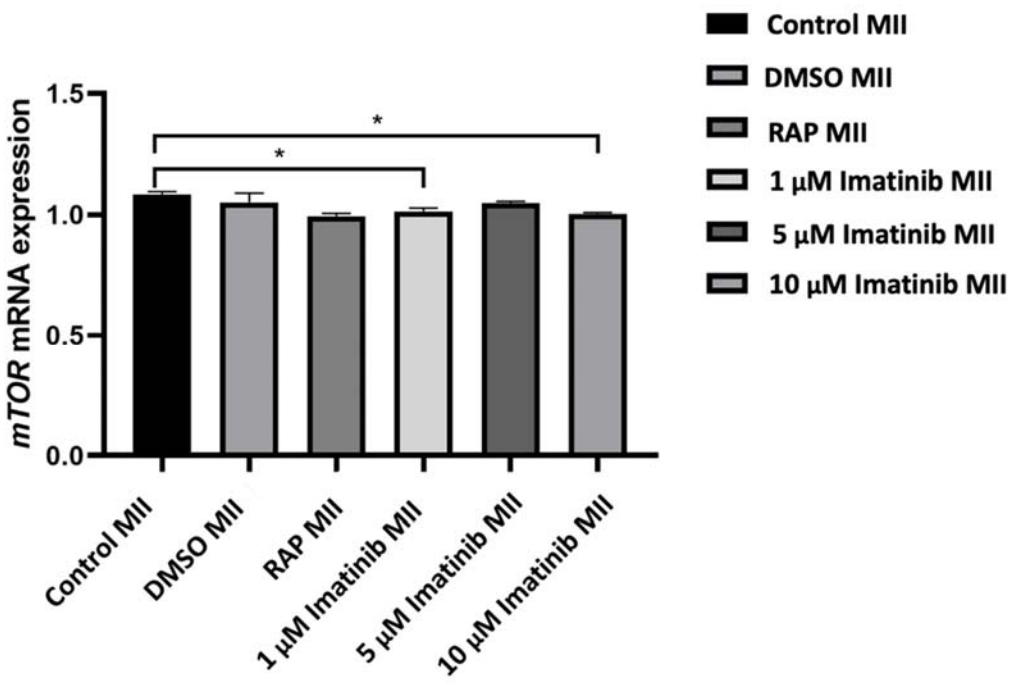

Figure 4.3.3. *mTOR* expression level in control, DMSO, 1000 μM rapamycin, 1 μM imatinib, 5 μM imatinib and 10 μM imatinib treatment at MII oocyte. Error bars indicate the SEM. n=3. (*p<0.1).

qRT-PCR results show the mRNA expression level of *c-Abl* in mouse GV oocytes in all the experimental groups. Compared with the control group, *c-Abl* expression level was significantly decreased in 1 μM and 5 μM imatinib treatment groups (**p<0.01) (Figure 4.3.4).

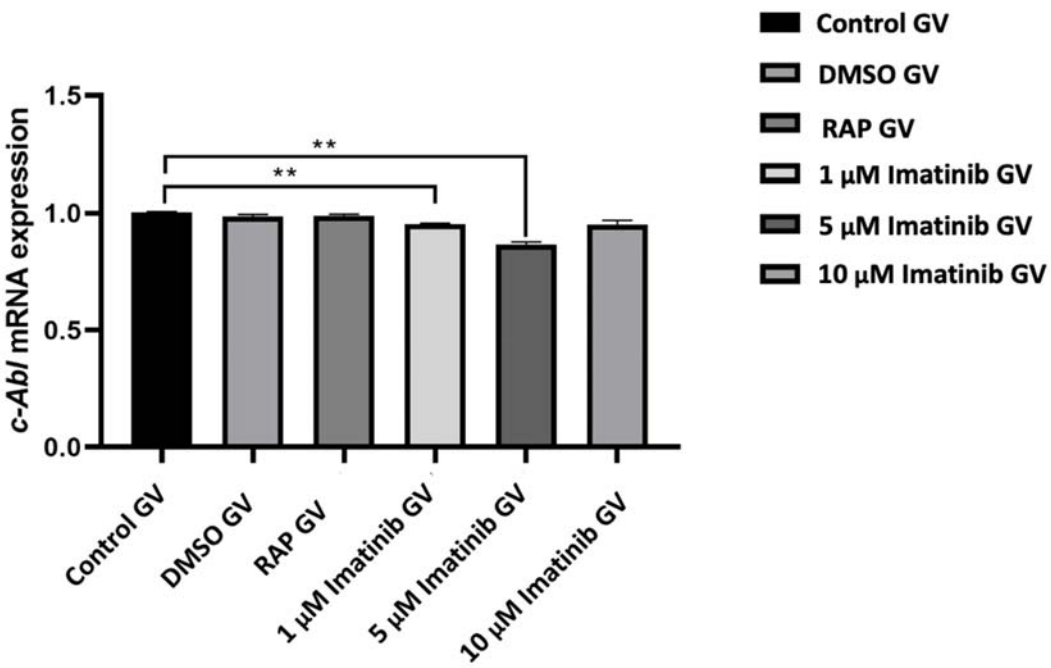

Figure 4.3.4. *c-Abl* expression level in control, DMSO, 1000 μM rapamycin, 1 μM imatinib, 5 μM imatinib and 10 μM imatinib treatment at GV oocyte. Error bars indicate the SEM. n=3. (**p<0.01).

qRT-PCR results show the mRNA expression level of *c-Abl* in mouse MI oocytes in all the experimental groups. There is no statistical difference between experimental groups at MI oocyte for *c-Abl* expression (Figure 4.3.5).

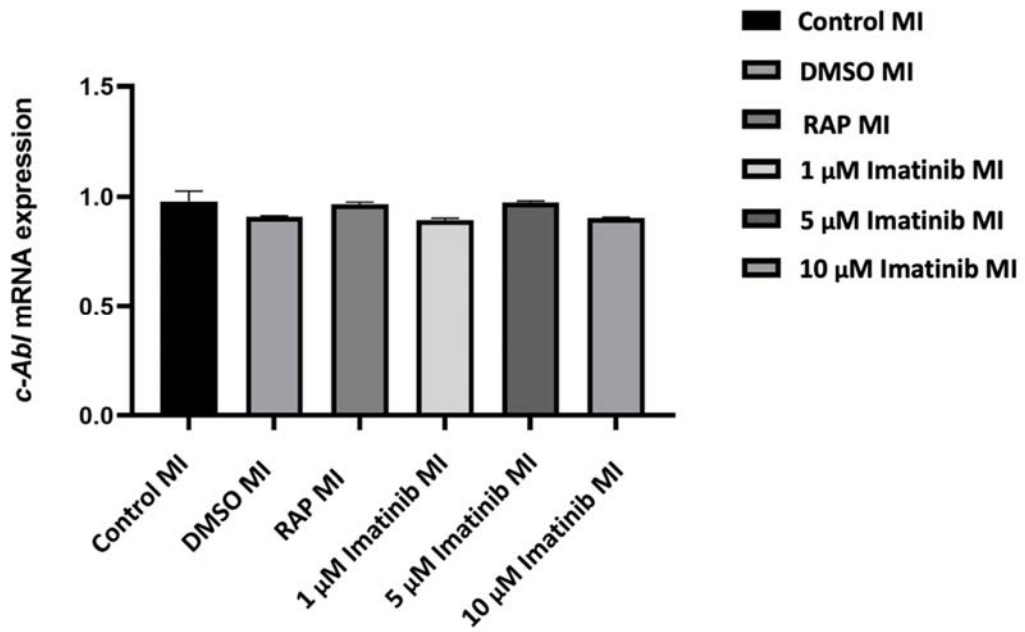

Figure 4.3.5. *c-Abl* expression level in control, DMSO, 1000 μM rapamycin, 1 μM imatinib, 5 μM imatinib and 10 μM imatinib treatment at MI oocyte. n=3.

qRT-PCR results show mRNA expression level of *c-Abl* in mouse MII oocytes in all the experimental groups. Compared with the control group, *c-Abl* expression was significantly decreased in the 1000 μM rapamycin treatment group. The expression level was further decreased after 1 μM and 5 μM imatinib treatment groups (*$p<0.1$) (Figure 4.3.6).

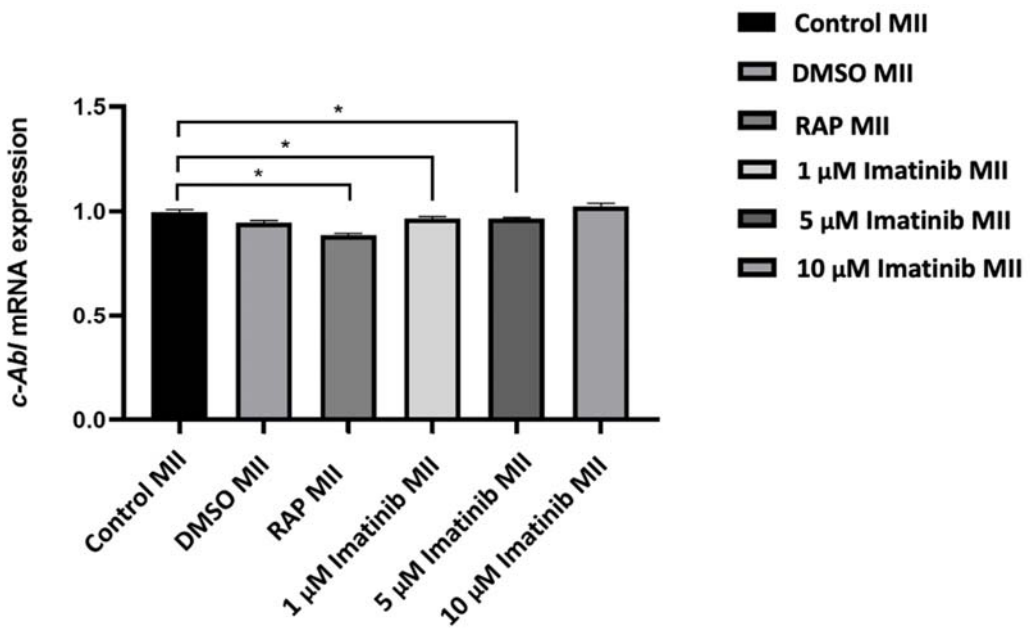

Figure 4.3.6. *c-Abl* expression level in control, DMSO, 1000 μM rapamycin, 1 μM imatinib, 5 μM imatinib and 10 μM imatinib treatment at MII stage mouse oocyte. Error bars indicate the SEM. n=3. (*p<0.1).

qRT-PCR results show the comparison of the mRNA expression levels of *c-Abl* and *mTOR* in mouse GV oocytes in all the experimental groups. In the rapamycin group, *mTOR* expression level was significantly increased compared to *c-Abl* expression level (**p<0.01). In the 1 μM imatinib group, *mTOR* mRNA expression level was significantly increased compared to *c-Abl* mRNA expression level (*p<0.1). In the 5 μM imatinib group, *mTOR* expression level was significantly increased compared to *c-Abl* expression level (****p<0.0001). In the 10 μM imatinib group, *mTOR* expression level was significantly increased compared to *c-Abl* expression level (***p<0.001). The *mTOR* expression level in the rapamycin group was significantly increased compared to the *c-Abl* expression level in the 5 μM imatinib group (****p<0.0001). The *mTOR* expression level in the 5 μM imatinib group was significantly increased compared to the *c-Abl* expression level in the 10 μM imatinib group (*p<0.1). The *mTOR* expression level in the rapamycin group was significantly increased compared to the *c-Abl* expression level in the control group (**p<0.01). The *mTOR* expression level in the control group was significantly increased compared to the *c-Abl* expression level in the 5 μM imatinib group (*p<0.1). The *mTOR* expression level in the 10 μM imatinib group was significantly

increased compared to the *c-Abl* expression level in the control group (*p<0.1) (Figure 4.3.7).

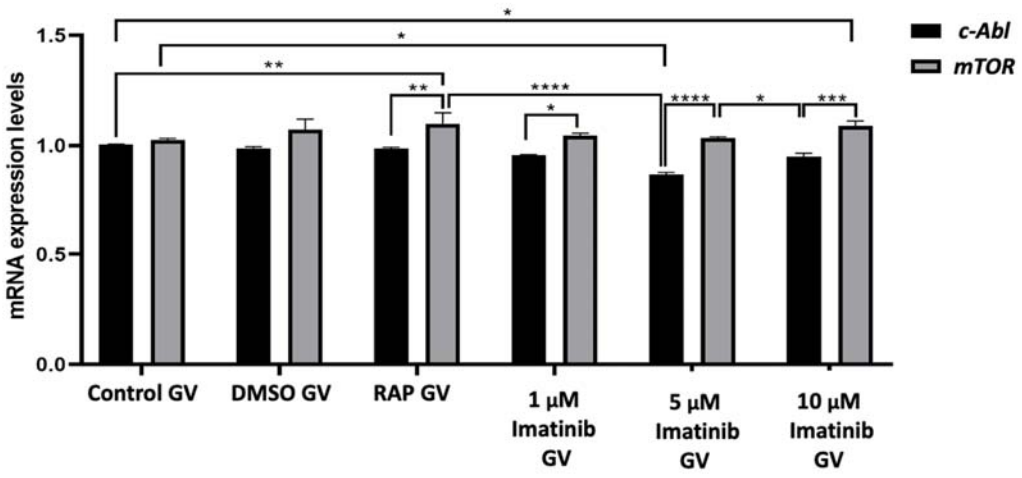

Figure 4.3.7. Comparision of *c-Abl* and *mTOR* expression in control, DMSO, 1000 μM rapamycin, 1 μM imatinib, 5 μM imatinib and 10 μM imatinib treatment at GV stage mouse oocyte (*p<0.1, **p<0.01, ***p<0.001, ****p<0.0001).

qRT-PCR results show the comparison of the mRNA levels of *c-Abl* and *mTOR* in mouse MI stage oocytes in all the experimental groups. In rapamycin group, *mTOR* expression level was significantly increased compared to *c-Abl* expression level (**p<0.01). In the 1 μM imatinib group, *mTOR* mRNA expression level was significantly increased compared to *c-Abl* expression level (*p<0.1). In the 5 μM imatinib group, *mTOR* expression level was significantly increased compared to *c-Abl* expression level (*p<0.1). In the 10 μM imatinib group, *mTOR* expression level was significantly increased compared to *c-Abl* expression level (*p < 0.1). The *mTOR* mRNA expression level in the rapamycin group was significantly increased compared to the *c-Abl* mRNA expression level in the 1 μM imatinib group and control group (***p<0.001, *p < 0.1). The *mTOR* mRNA expression level in the control group was significantly increased compared to the *c-Abl* mRNA expression level in the 1 μM imatinib group and in the 10 μM imatinib group (**p<0.01, **p<0.01). The *mTOR* mRNA expression level in the 5 μM imatinib group was significantly increased compared to the *c-Abl* mRNA expression level in the control group (*p<0.1) (Figure 4.3.8).

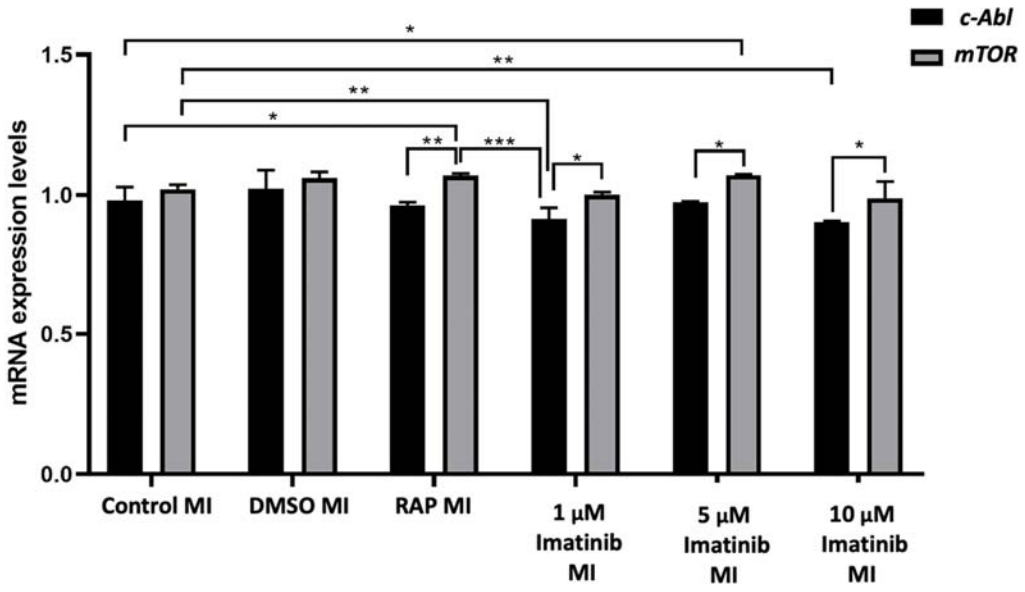

Figure 4.3.8. Comparison of *c-Abl* and *mTOR* expression in control, DMSO, 1000 μM rapamycin, 1 μM imatinib, 5 μM imatinib and 10 μM imatinib treatment at MI stage mouse oocyte (*p<0.1, **p<0.01, ***p<0.001).

qRT-PCR results show the comparison of the mRNA levels of *c-Abl* and *mTOR* in mouse MII stage oocytes in all the experimental groups. In the rapamycin group, *mTOR* expression level was significantly increased compared to *c-Abl* expression level (****p<0.0001). In the 1 μM imatinib group and 10 μM imatinib group, no statistical difference between *mTOR* and *c-Abl* mRNA expression levels. In the 5 μM imatinib group, *mTOR* expression level was significantly increased compared to *c-Abl* expression level (**p<0.01). The *mTOR* expression level in the 5 μM imatinib group was significantly increased compared to the *c-Abl* expression level in the 1 μM imatinib group and control group (**p<0.01, *p<0.1). The *mTOR* expression level in the control group was significantly increased compared to the *c-Abl* expression level in the rapamycin group, 1 μM imatinib group, 5 μM imatinib group and 10 μM imatinib group (****p<0.0001, ****p<0.0001, ****p<0.0001, **p<0.01) (Figure 4.3.9).

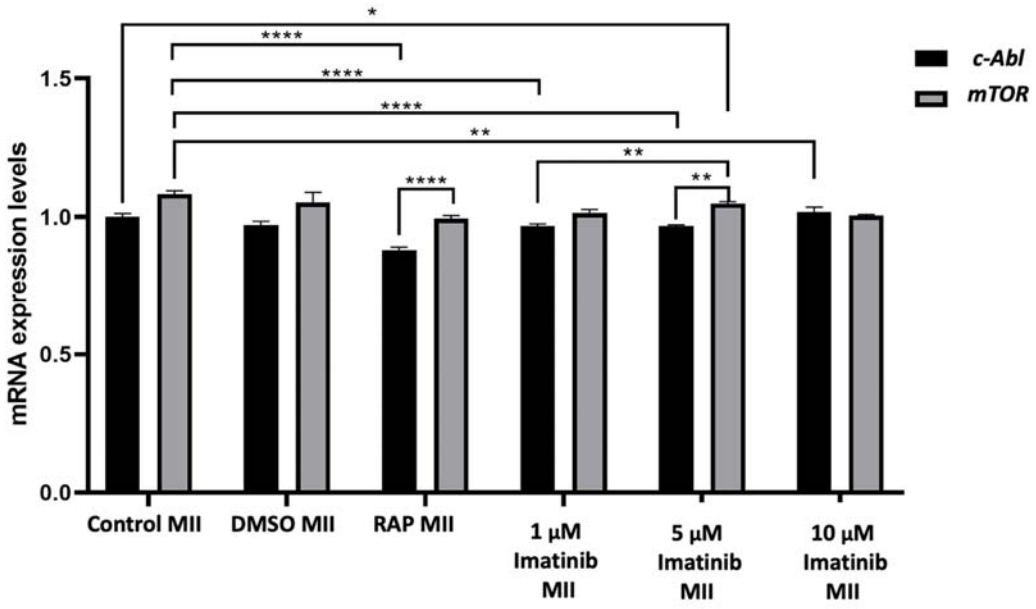

Figure 4.3.9. Comparison of *c-Abl* and *mTOR* expression in control, DMSO, 1000 µM rapamycin, 1 µM imatinib, 5 µM imatinib and 10 µM imatinib treatment at MII stage mouse oocyte. (*p<0.1, **p<0.01, ****p<0.0001).

5. DISCUSSION and CONCLUSION

The quality of the oocytes is one of the most important factors that help pregnancy, as high-quality oocytes lead to a high-quality embryo that is more likely to implantation and continue the pregnancy[52]. The question remains: how do we get a good quality oocyte? Oocyte maturation is a complex and precisely coordinated set of processes that result in nuclear and cytoplasmic changes that generate mature, high-quality oocytes[4]. Thus, the higher the competence of the oocyte maturation process, the higher the quality of the oocyte[109]. Thereby, there is a pressing need to understand the molecular mechanisms that play a role in the maturation process and constitute the biological competence of oocytes, as these mechanisms are not still understood very well. In this study, we aimed to show the role of *mTOR* and *c-Abl* and the relationship between them during the process of oocyte maturation.

We have defined the process of oocyte maturation as the process during which a primordial follicle develops into an antral follicle that resumes its meiosis I (MI) from the diplotene stage arrest that had begun almost before birth, leading to the breakdown of the germinal vesicle, MS formation, extrusion of the PBI, rearrangement of the cortical cytoskeleton, and the entry into the meiosis II. Thus, a haploid oocyte capable of fertilization is formed[8].

mTOR supports follicle development starting from stimulating primordial follicle growth and up oocyte formation[25]. *mTOR* controls cell growth by producing proteins (mRNA translation), through modifications of phosphorylation and stimulation of transcription of ribosomal RNA, which stimulates ribosome biogenesis[82]. During meiotic maturation, mTORC1 localizes on the MS and condenses around chromosomes and regulates chromosomal alignment and its segregation[24].

c-Abl repairs DNA double-strand breaks (DSBs) that naturally occur during meiosis and mitosis or when exposed to external factors such as radiation or endogenous factors such as oxidative stress and thus maintain genomic integrity in the oocyte[29]. *c-Abl* inhibits the telomerase enzyme by phosphorylation the TERT catalyst unit, which leads to shortening of the telomeres, thus stimulating apoptosis, and thereby preventing the formation of tumors[95]. Also, it plays a role in regulating the cytoskeleton of F-actin. So, it supports meiotic maturation by regulating the mechanism of spindle action and correct separation of chromosomes[30].

A study suggested a possible interaction between tumor protein (p53) and *mTOR* is the tyrosine kinase *c-Abl*, which interacts with p53 and phosphorylates *mTOR* on tyrosine residues[34]. *c-Abl* inhibits the kinase activity of *mTOR*[35].

To investigate the roles of *mTOR* and *c-Abl* in the process of oocyte maturation, we treated GV oocytes with 2 different treatment groups as imatinib (inhibitor of *c-Abl*, 1 μM, 5 μM and 10 μM) and rapamycin (inhibitor of mTORC1, 1000 μM). Then, we recorded the rate of GV, MI and MII after 16 h culture, imaged and scored based on 6 parameters. Also, we detected *mTOR* and *c-Abl* mRNA expression levels at GV, MI and MII oocyte stages in all experimental groups by quantitative RT-PCR and then we performed a comparison of *mTOR* and *c-Abl* mRNA expression levels at GV, MI and MII oocyte stages in all experimental groups.

In the rapamycin group, we observed that the percentage of GV and MI oocytes did not differ significantly from that in the control and DMSO groups. While the percentage of MII oocytes slightly increased compared to that in the control and DMSO groups. Rapamycin had a slightly negative effect on the morphology of GV, MI and MII oocytes. Interestingly, the qRT-PCR results showed that the mRNA expression levels of *mTOR* in GV, MI and MII oocytes in the rapamycin group did not decrease. At this point, we suggested that after 1000 μM rapamycin treatment, changes have occurred at the protein level.

In contrast, a previous study demonstrated that 10 μM, and 50 μM rapamycin treatment of aged porcine oocytes in vitro significantly increased the maturation rate, decreased *mTOR* gene expression, and rescued aberrant spindle regulation and chromosomal misalignment[110]. Also in another study, treatment of mouse oocytes with 10 μM rapamycin increased developmental competence, mitochondrial membrane potential, spindle/chromosome integrity and normal cortical granule distribution[111]. However, another study showed that treatment of mouse oocytes with 10 μM rapamycin reduced *mTOR* at the RNA and protein levels, altered asymmetric division and disrupted actin cap formation and cortical granule-free domain, causing failure of spindle migration. mTORC2 is the protein that plays a role in actin regulation and is insensitive to rapamycin, but studies have shown that prolonged exposure to rapamycin in culture medium inhibits mTORC2 and leads to failure of actin regulation[112]. This may be the reason for the decreased quality of rapamycin-treated oocytes in our study as well. Also, a study showed that 1 nM rapamycin treatment of bovine oocytes increased the maturation rate, while doses of 10 nM and 100 nM decreased the maturation rate[113]. However,

another study showed that 10 nM of rapamycin of mice oocytes increased the maturation rate and improved the quality by promoting DNA repair during in vitro maturation[114]. Treatment of mouse oocytes with 2 nM rapamycin also significantly increased autophagy- and apoptosis-related gene expression, oxidative stress, apoptosis rates, abnormal mitochondrial redistribution, and significantly decreased oocyte first polar body extrusion (PBE) rates, spindle/chromosome integrity and developmental competence[115]. And in another study, treatment of mouse oocytes with 50 nM rapamycin also significantly increased apoptosis rate[116]. One study showed that the autophagy activity was low in poor-quality bovine oocytes and that treatment with 100 nM of rapamycin increased that activity and thus increased the developmental competence[117]. Also, in porcine oocytes, 1 nM, 5 nM and 10 nM rapamycin increased the rate of maturation by stimulating autophagy[118]. While Treatment of Rana dybowskii oocytes with 1 nM, 10 nM and 100 nM rapamycin inhibited GVBD by inhibiting S6 kinase[119].

The results of these studies indicated that rapamycin has a dose-dependent effect. Not only that, but the use of the same dose showed contradictory results between studies, which indicates that many hidden mechanisms affect the action of rapamycin. Therefore, before using rapamycin to treat human oocytes, researchers must conduct more studies to better understand the safe dose of the rapamycin and avoid the risks that may damage the embryo.

In the 1 μM imatinib group, we observed that the percentage of GV oocytes slightly increased compared to that in the control and DMSO groups. While the percentage of MI and MII oocytes slightly decreased compared to that in the control and DMSO groups. 1 μM imatinib had a slightly negative effect on the morphology of GV, no negative effect on the morphology of MI oocytes and a negative effect on the morphology of MII oocytes. In the 5μM imatinib group, we observed that the percentage of GV oocytes increased compared to that in the control and DMSO groups. While the percentage of MI and MII oocytes decreased compared to that in the control and DMSO groups. 5 μM imatinib had a slightly negative effect on the morphology of GV and MI and a negative effect on the morphology of MII oocytes. In the 10 μM imatinib group, we observed that the percentage of GV oocytes did not differ significantly from that in the control and DMSO groups. While the percentage of MI oocytes greatly increased and the percentage of MII oocytes greatly decreased compared to that in the control and DMSO groups. 10 μM imatinib had a great negative effect on the morphology of GV, MI and MII oocytes. The qRT-PCR results showed that the mRNA expression levels of *c-*

Abl in GV significantly decreased in 1 μM and 5 μM imatinib treatment groups. There is no statistical difference between imatinib groups, control and DMSO groups at MI stage oocyte. mRNA expression levels of *c-Abl* in MII oocyte significantly decreased in 1 μM and 5 μM imatinib treatment groups. Also, mRNA expression levels of *c-Abl* in the 10 μM imatinib treatment group did not decrease. At this point, we suggested that after 10 μM imatinib treatment, changes have occurred at the protein level.

There have been no previous studies exploring the effect of c-Abl during in vitro oocyte maturation while much research has been done in vivo or on in vitro ovarian tissue for the inhibition of *c-Abl* by imatinib in conjunction with cancer therapy. In our study, we demonstrated that imatinib reduced the rate of oocyte maturation and significantly affected their quality on dose-dependent; while in cancer patients, it gave an opposite result, as it resulted in protecting the ovarian reserve and preventing premature ovarian failure[120-122]. A study demonstrated that administration of imatinib in mice treated with cisplatin also rescued abnormal spindle organization and improved the rate of in vitro fertilization[123]. While another study showed that it increased the number of primary and secondary follicles but resulted in fewer total cells in the blastocyst and a significant shift from the inner cell mass to trophectoderm cells[124]. In the light of literature, the mechanism by which imatinib protects the oocytes is not fully understood[120]. Therefore more studies are needed to understand the role of *c-Abl* in oocyte and early embryonic development.

A study demonstrated that *mTOR* inhibition led to the sustained activation of c-Jun N-terminal kinases (JNK) and this helps *c-Abl* cross over into the nucleus to repair DNA damage[99]. Thereby *mTOR* inhibition is essential for DNA repair with *c-Abl*. Another study suggested that there is a relationship between *mTOR* and c-Abl and that c-Abl inhibits *mTOR*[34,35]. In our study, we were able to prove this relationship in mouse oocytes, as the qRT-PCR results that compared the mRNA expression levels of *mTOR* and *c-Abl* in the GV, MI and MII oocyte stages in all treatment groups showed that *c-Abl* inhibition led to an increase in *mTOR* expression in GV and MI oocytes in 1 μM, 5 μM and 10 μM imatinib treated groups, while in MII oocytes *c-Abl* inhibition increased *mTOR* mRNA level only in 5 μM imatinib group.

Several studies have demonstrated that overactivity of *mTOR* leads to stimulation of follicular development, since *mTOR* leads to premature activation of primordial follicles, thus follicular depletion and premature ovarian failure (POF) and that *mTOR* inhibition with rapamycin preserved primordial follicles and prevented POF[125-128]. Several studies have proven that imatinib treatment in cancer patients was not able to

protect ovarian reserves from depletion[129,130]. Based on our study in which we demonstrated the relationship between mTOR and c-Abl, we can attribute the depletion of oocytes to the overactivity of *mTOR*. When imatinib inhibits c-Abl, *mTOR* activity increases, leading to depletion of ovarian reserves. Therefore, we suggested that the use of imatinib as a treatment to preserve ovarian reserve in women undergoing chemotherapy is still controversial.

After GVBD, all of the oocytes cannot complete their maturation and they cannot release their first polar body, which is necessary to complete the nuclear maturation of the oocyte. Protein synthesis is important in the transition of oocytes from the germinal vesicle stage to MII and in maintaining its arrest in the MII stage so that blocking protein synthesis in the oocyte prevents activation of oocyte maturation. In our study, after rapamycin treatment and imatinib treatment we did not observe a dramatic decrease in *mTOR* and *c-Abl* at the transcriptional level, respectively. Therefore, the changes reflected in the oocyte morphology may not have been determined at the transcriptional level. To reveal the role of *c-Abl* and *mTOR* in oocyte maturation, we suggested that new studies should be designed to get information at the translational level.

The molecular basis of the mechanisms that interrupt meiosis in the oocyte has not been fully elucidated. In conclusion, understanding the roles of *c-Abl* and *mTOR* during oocyte maturation will help us improve oocyte and embryo quality, and we believe that understanding the relationship between *c-Abl* and *mTOR* opens new horizons for us to know the best ways to protect fertility in cancer patients.

6. REFERENCES

1. Keefe D, Kumar M, Kalmbach KJF, Sterility. Oocyte competency is the key to embryo potential. 2015;103(2):317-322.
2. Loutradis D, Kiapekou E, Zapanti E, Antsaklis AJAotNYAoS. Oocyte maturation in assisted reproductive techniques. 2006;1092(1):235-246.
3. Da Broi M, Giorgi V, Wang F, et al. Influence of follicular fluid and cumulus cells on oocyte quality: clinical implications. 2018;35(5):735-751.
4. Tukur HA, Aljumaah RS, Swelum AA-A, Alowaimer AN, Saadeldin IMJJoAR, Biotechnology. The making of a competent oocyte–a review of oocyte development and its regulation. 2020;35(1):2-11.
5. Fan H-Y, Sun Q-Y. Oocyte meiotic maturation. *The Ovary*. Elsevier; 2019:181-203.
6. Wołodko K, Castillo-Fernandez J, Kelsey G, Galvão AJIjoms. Revisiting the impact of local leptin signaling in folliculogenesis and oocyte maturation in obese mothers. 2021;22(8):4270.
7. Hatırnaz Ş, Hatırnaz ES, Kaya AE, et al. Oocyte maturation abnormalities-A systematic review of the evidence and mechanisms in a rare but difficult to manage fertility pheneomina. 2022;19(1):60.
8. Pan B, Li JJRB, Endocrinology. The art of oocyte meiotic arrest regulation. 2019;17(1):1-12.
9. Firmani LD, Uliasz TF, Mehlmann LMJDB. The switch from cAMP-independent to cAMP-dependent arrest of meiotic prophase is associated with coordinated GPR3 and CDK1 expression in mouse oocytes. 2018;434(1):196-205.
10. Li J, Qian W-P, Sun Q-YJBoR. Cyclins regulating oocyte meiotic cell cycle progression. 2019;101(5):878-881.
11. Verlhac M-H, Terret M-EJF. Oocyte maturation and development. 2016;5
12. Kirillova A, Smitz JE, Sukhikh GT, Mazunin IJC. The role of mitochondria in oocyte maturation. 2021;10(9):2484.
13. Adhikari D, Lee I-w, Yuen WS, Carroll JJBoR. Oocyte mitochondria—key regulators of oocyte function and potential therapeutic targets for improving fertility. 2022;106(2):366-377.
14. Duan X, Sun S-CJBoR. Actin cytoskeleton dynamics in mammalian oocyte meiosis. 2019;100(1):15-24.
15. Trebichalská Z, Kyjovská D, Kloudová S, Otevřel P, Hampl A, Holubcová ZJBor. Cytoplasmic maturation in human oocytes: an ultrastructural study. 2021;104(1):106-116.
16. Reyes JM, Ross PJJWIRR. Cytoplasmic polyadenylation in mammalian oocyte maturation. 2016;7(1):71-89.
17. Susor A, Kubelka MJO. Translational regulation in the mammalian oocyte. 2017:257-295.
18. Watson AJJoas. Oocyte cytoplasmic maturation: a key mediator of oocyte and embryo developmental competence. 2007;85(suppl_13):E1-E3.
19. Gindi N, Grossman H, Bar-Joseph H, et al. Fyn and argonaute 2 participate in maternal-mRNA degradation during mouse oocyte maturation. 2022;21(8):792-804.
20. Prather RS, Ross JW, Isom SC, Green JAJSoR, supplement F. Transcriptional, post-transcriptional and epigenetic control of porcine oocyte maturation and embryogenesis. 2009;66:165.

21. He M, Zhang T, Yang Y, Wang CJFic, biology d. Mechanisms of oocyte maturation and related epigenetic regulation. 2021;9
22. Guo J, Zhang T, Guo Y, et al. Oocyte stage-specific effects of MTOR determine granulosa cell fate and oocyte quality in mice. 2018;115(23):E5326-E5333.
23. Sánchez F, Smitz JJBeBA-MBoD. Molecular control of oogenesis. 2012;1822(12):1896-1912.
24. Guo Z, Yu QJFie. Role of mTOR signaling in female reproduction. 2019:692.
25. Sobinoff AP, Sutherland JM, Mclaughlin EAJMBsorm. Intracellular signalling during female gametogenesis. 2013;19(5):265-278.
26. Zhang T, He M, Zhao L, et al. HDAC6 regulates primordial follicle activation through mTOR signaling pathway. 2021;12(6):1-12.
27. Papageorgiou K, Mastora E, Zikopoulos A, Grigoriou ME, Georgiou I, Michaelidis TMJFiE. Interplay Between mTOR and Hippo Signaling in the Ovary: Clinical Choice Guidance Between Different Gonadotropin Preparations for Better IVF. 2021:883.
28. Estienne A, Bongrani A, Ramé C, et al. Energy sensors and reproductive hypothalamo-pituitary ovarian axis (HPO) in female mammals: Role of mTOR (mammalian target of rapamycin), AMPK (AMP-activated protein kinase) and SIRT1 (Sirtuin 1). 2021;521:111113.
29. Gonfloni SJO. DNA damage stress response in germ cells: role of c-Abl and clinical implications. 2010;29(47):6193-6202.
30. Mutluay D, Hakan ÖJAÜVFD. Relationships between Abelson tyrosine kinase (c-abl) and spindle during meiotic division in mouse oocyte in vitro. 2018;66(1):89-93.
31. Vallet N, Boissel N, Elefant E, et al. Can Some Anticancer Treatments Preserve the Ovarian Reserve? 2021;26(6):492-503.
32. Yaba A, Agus S, Yıldırım E, Erdogan CS, Yılmaz BJJoR, Transduction S. Interaction of the mTERT telomerase catalytic subunit with the c-Abl tyrosine kinase in mouse granulosa cells. 2020;40(4):365-373.
33. Xiong J, Xue L, Li Y, et al. THERAPY OF ENDOCRINE DISEASE: Novel protection and treatment strategies for chemotherapy-associated ovarian damage. 2021;184(5):R177-R192.
34. Sabatini D, Gingras A-C, Kumar M, et al. Regulation of the rapamycin and FKBP-target 1/mammalian target of rapamycin and cap-dependent initiation of translation by the c-Abl protein-tyrosine kinase. 2000;275(15):10779-10787.
35. Proud CGJDr. The multifaceted role of mTOR in cellular stress responses. 2004;3(8-9):927-934.
36. Gibson E, Mahdy H. Anatomy, abdomen and pelvis, ovary. 2019;
37. Hoare BS, Khan YS. Anatomy, abdomen and pelvis, female internal genitals. *StatPearls [Internet]*. StatPearls Publishing; 2021.
38. Holesh J, Bass A, Lord MJSTISP. Physiology, ovulation.[Updated 2020 Aug 22]. 2021;
39. Kirkendoll SD, Bacha D. Histology, Corpus Albicans. *StatPearls [Internet]*. StatPearls Publishing; 2021.
40. Silvestris E, De Palma G, Canosa S, et al. Human ovarian cortex biobanking: a fascinating resource for fertility preservation in cancer. 2020;21(9):3245.
41. Heeren AM, Van Iperen L, Klootwijk DB, et al. Development of the follicular basement membrane during human gametogenesis and early folliculogenesis. 2015;15(1):1-13.
42. Baerwald AR, Adams GP, Pierson RAJHru. Ovarian antral folliculogenesis during the human menstrual cycle: a review. 2012;18(1):73-91.

43. Cox E, Takov V. Embryology, ovarian follicle development. *StatPearls [Internet]*. StatPearls Publishing; 2021.
44. Waters M, Tadi P. Genetics, Female Gametogenesis. *StatPearls [Internet]*. StatPearls Publishing; 2021.
45. Williams CJ, Erickson GF. Morphology and Physiology of the Ovary. 2015;
46. Rimon-Dahari N, Yerushalmi-Heinemann L, Alyagor L, Dekel NJMmocdigd. Ovarian folliculogenesis. 2016:167-190.
47. Hutt KJ, Albertini DFJRbo. An oocentric view of folliculogenesis and embryogenesis. 2007;14(6):758-764.
48. Silva J, Figueiredo J, Van den Hurk RJT. Involvement of growth hormone (GH) and insulin-like growth factor (IGF) system in ovarian folliculogenesis. 2009;71(8):1193-1208.
49. Mihajlović AI, FitzHarris GJCB. Segregating chromosomes in the mammalian oocyte. 2018;28(16):R895-R907.
50. Balaban B, Urman BJRbo. Effect of oocyte morphology on embryo development and implantation. 2006;12(5):608-615.
51. Serhal P, Ranieri D, Kinis A, Marchant S, Davies M, Khadum IJHr. Oocyte morphology predicts outcome of intracytoplasmic sperm injection. 1997;12(6):1267-1270.
52. Wang Q, Sun Q-YJR, Fertility, Development. Evaluation of oocyte quality: morphological, cellular and molecular predictors. 2006;19(1):1-12.
53. Rienzi L, Balaban B, Ebner T, Mandelbaum JJHR. The oocyte. 2012;27(suppl_1):i2-i21.
54. Tilia L, Chapman M, Kilani S, Cooke S, Venetis CJF, Sterility. Oocyte meiotic spindle morphology is a predictive marker of blastocyst ploidy—a prospective cohort study. 2020;113(1):105-113. e1.
55. Ebner T, Moser M, Tews GJRbo. Is oocyte morphology prognostic of embryo developmental potential after ICSI? 2006;12(4):507-512.
56. Rienzi L, Ubaldi F, Martinez F, et al. Relationship between meiotic spindle location with regard to the polar body position and oocyte developmental potential after ICSI. 2003;18(6):1289-1293.
57. Tripathi A, Kumar KP, Chaube SKJJocp. Meiotic cell cycle arrest in mammalian oocytes. 2010;223(3):592-600.
58. Li R, Albertini DFJNrMcb. The road to maturation: somatic cell interaction and self-organization of the mammalian oocyte. 2013;14(3):141-152.
59. Adhikari D, Liu KJM, endocrinology c. The regulation of maturation promoting factor during prophase I arrest and meiotic entry in mammalian oocytes. 2014;382(1):480-487.
60. Gutnisky C, Morado S, Gadze T, et al. Morphological, biochemical and functional studies to evaluate bovine oocyte vitrification. 2020;143:18-26.
61. MacLennan M, Crichton JH, Playfoot CJ, Adams IR. Oocyte development, meiosis and aneuploidy. Elsevier; 2015:68-76.
62. Severson AF, von Dassow G, Bowerman BJCtidb. Oocyte meiotic spindle assembly and function. 2016;116:65-98.
63. Mogessie B, Scheffler K, Schuh MJARoC, Biology D. Assembly and positioning of the oocyte meiotic spindle. 2018;34:381-403.
64. Mira AJJotb. Why is meiosis arrested? 1998;194(2):275-287.
65. Sen A, Severance AL. Oogenesis & Ovulation: Oocyte Maturation and Ovulation, Comparative. 2018;

66. Liu L, Kong N, Xia G, Zhang MJR, Fertility, Development. Molecular control of oocyte meiotic arrest and resumption. 2013;25(3):463-471.
67. Rodriguez KF, Farin CEJR, Fertility, Development. Gene transcription and regulation of oocyte maturation. 2003;16(2):55-67.
68. Sirait B, Wiweko B, Jusuf AA, Iftitah D, Muharam RJFiC, Biology D. Oocyte Competence Biomarkers Associated With Oocyte Maturation: A Review. 2021;9
69. Sen A, Caiazza FJFB. Oocyte maturation: a story of arrest and release. 2013;5(5):451-477.
70. Veeck LLJAotNYAoS. Oocyte assessment and biological performance. 1988;541(1):259-274.
71. Coticchio G, Dal Canto M, Mignini Renzini M, et al. Oocyte maturation: gamete-somatic cells interactions, meiotic resumption, cytoskeletal dynamics and cytoplasmic reorganization. 2015;21(4):427-454.
72. Combelles C, Cekleniak N, Racowsky C, Albertini DJHR. Assessment of nuclear and cytoplasmic maturation in in-vitro matured human oocytes. 2002;17(4):1006-1016.
73. Babayev E, Seli EJCoio, gynecology. Oocyte mitochondrial function and reproduction. 2015;27(3):175.
74. Lin T, Lee JE, Kang JW, Shin HY, Lee JB, Jin DIJIJoMS. Endoplasmic reticulum (ER) stress and unfolded protein response (UPR) in mammalian oocyte maturation and preimplantation embryo development. 2019;20(2):409.
75. Wakelam MJ, Mikoshiba K. The IP3 receptor/Ca2+ channel and its cellular function. Portland Press; 2007:9-22.
76. Mao L, Lou H, Lou Y, Wang N, Jin FJRBO. Behaviour of cytoplasmic organelles and cytoskeleton during oocyte maturation. 2014;28(3):284-299.
77. Mendez R, Richter JDJNrMcb. Translational control by CPEB: a means to the end. 2001;2(7):521-529.
78. Hua H, Kong Q, Zhang H, et al. Targeting mTOR for cancer therapy. 2019;12(1):1-19.
79. Dibble CC, Manning BDJNcb. Signal integration by mTORC1 coordinates nutrient input with biosynthetic output. 2013;15(6):555-564.
80. Laplante M, Sabatini DMJJocs. mTOR signaling at a glance. 2009;122(20):3589-3594.
81. Jacinto E, Loewith R, Schmidt A, et al. Mammalian TOR complex 2 controls the actin cytoskeleton and is rapamycin insensitive. 2004;6(11):1122-1128.
82. Wang X, Proud CGJP. The mTOR pathway in the control of protein synthesis. 2006;21(5):362-369.
83. Adhikari D, Liu KJCC. mTOR signaling in the control of activation of primordial follicles. Taylor & Francis; 2010. p. 1673-1674.
84. Shen M, Jiang Y, Guan Z, et al. Protective mechanism of FSH against oxidative damage in mouse ovarian granulosa cells by repressing autophagy. 2017;13(8):1364-1385.
85. Su Y-Q, Yin Y, Guo J, Gong X, Tian Y, Shi LJBoR. MTOR-mediated interaction between the oocyte and granulosa cells regulates the development and function of both compartments in mice. 2022;
86. Zhao Y, Feng H, Zhang Y, et al. Current understandings of core pathways for the activation of mammalian primordial follicles. 2021;10(6):1491.
87. Colicelli JJSs. ABL tyrosine kinases: evolution of function, regulation, and specificity. 2010;3(139):re6-re6.

88. Wang G-F, Dong Q, Bai Y, et al. c-Abl kinase-mediated phosphorylation of γ-tubulin promotes γ-tubulin ring complexes assembly and microtubule nucleation. 2022;298(4)
89. Wang JYJM, biology c. The capable ABL: what is its biological function? 2014;34(7):1188-1197.
90. Bohio AA, Wang R, Zeng X, Ba XJMMR. c-Abl-mediated tyrosine phosphorylation of DNA damage response proteins and implications in important cellular functions. 2020;22(2):612-619.
91. Taagepera S, McDonald D, Loeb JE, et al. Nuclear-cytoplasmic shuttling of C-ABL tyrosine kinase. 1998;95(13):7457-7462.
92. Woodring PJ, Litwack ED, O'Leary DD, Lucero GR, Wang JY, Hunter TJTJocb. Modulation of the F-actin cytoskeleton by c-Abl tyrosine kinase in cell spreading and neurite extension. 2002;156(5):879-892.
93. Baskaran R, Dahmus ME, Wang JJPotNAoS. Tyrosine phosphorylation of mammalian RNA polymerase II carboxyl-terminal domain. 1993;90(23):11167-11171.
94. Yoshida K, Miki YJCc. Enabling death by the Abl tyrosine kinase: mechanisms for nuclear shuttling of c-Abl in response to DNA damage. 2005;4(6):777-779.
95. Kharbanda S, Kumar V, Dhar S, et al. Regulation of the hTERT telomerase catalytic subunit by the c-Abl tyrosine kinase. 2000;10(10):568-575.
96. Levav-Cohen Y, Goldberg Z, Zuckerman V, et al. C-Abl as a modulator of p53. 2005;331(3):737-749.
97. Mirabilii S, Ricciardi MR, Piedimonte M, Gianfelici V, Bianchi MP, Tafuri AJIjoms. Biological aspects of mTOR in leukemia. 2018;19(8):2396.
98. Budanov AV, Karin MJC. p53 target genes sestrin1 and sestrin2 connect genotoxic stress and mTOR signaling. 2008;134(3):451-460.
99. Mancini M, Corradi V, Petta S, Martinelli G, Barbieri E, Santucci MAJLr. mTOR inhibitor RAD001 (Everolimus) enhances the effects of imatinib in chronic myeloid leukemia by raising the nuclear expression of c-ABL protein. 2010;34(5):641-648.
100. Attoub S, Rivat C, Rodrigues S, et al. The c-kit tyrosine kinase inhibitor STI571 for colorectal cancer therapy. 2002;62(17):4879-4883.
101. Sims JT, Plattner RJCc, pharmacology. MTT assays cannot be utilized to study the effects of STI571/Gleevec on the viability of solid tumor cell lines. 2009;64(3):629-633.
102. Levy D, Adamovich Y, Reuven N, Shaul YJMc. Yap1 phosphorylation by c-Abl is a critical step in selective activation of proapoptotic genes in response to DNA damage. 2008;29(3):350-361.
103. Lazzaroni-Tealdi E, Barad DH, Albertini DF, et al. Oocyte scoring enhances embryo-scoring in predicting pregnancy chances with IVF where it counts most. 2015;10(12):e0143632.
104. Griffin J, Emery BR, Huang I, Peterson CM, Carrell DTJJoe, reproduction ca. Comparative analysis of follicle morphology and oocyte diameter in four mammalian species (mouse, hamster, pig, and human). 2006;3(1):1-9.
105. Wassarman PM, Josefowicz WJJJom. Oocyte development in the mouse: an ultrastructural comparison of oocytes isolated at various stages of growth and meiotic competence. 1978;156(2):209-235.
106. Liu X, Sun Y. Microfluidic devices for single-cell trapping and automated micro-robotic injection. *Microfluidic Devices for Biomedical Applications*. Elsevier; 2013:351-365e.

107. Jennings PC, Merriman JA, Beckett EL, Hansbro PM, Jones KTJHr. Increased zona pellucida thickness and meiotic spindle disruption in oocytes from cigarette smoking mice. 2011;26(4):878-884.
108. Fan ZQ, Wang YP, Yan CL, Suo L, Zhu SEJLa. Positive effect of partial zona pellucida digestion on in vitro fertilization of mouse oocytes with cryopreserved spermatozoa. 2009;43(1):72-77.
109. Krisher RJJoas. The effect of oocyte quality on development. 2004;82(suppl_13):E14-E23.
110. Lee SE, Kim EY, Choi HY, et al. Rapamycin rescues the poor developmental capacity of aged porcine oocytes. 2014;27(5):635.
111. Lin F-H, Zhang W-L, Li H, et al. Role of autophagy in modulating post-maturation aging of mouse oocytes. 2018;9(3):1-12.
112. Lee SE, Sun SC, Choi HY, Uhm SJ, Kim NHJMr, development. mTOR is required for asymmetric division through small GTPases in mouse oocytes. 2012;79(5):356-366.
113. Kordowitzki P, Hamdi M, Derevyanko A, Rizos D, Blasco MJA. The effect of rapamycin on bovine oocyte maturation success and metaphase telomere length maintenance. 2020;12(8):7576.
114. Yang Q, Xi Q, Wang M, et al. Rapamycin improves the quality and developmental competence of mice oocytes by promoting DNA damage repair during in vitro maturation. 2022;20(1):1-11.
115. Zhang Y, Li Q, Li W, et al. 2-Mercaptoethanol promotes porcine oocyte maturation in vitro by maintaining autophagy homeostasis. 2022;186:155-167.
116. Lobascio A, Klinger F, Scaldaferri M, Farini D, De Felici MJR. Analysis of programmed cell death in mouse fetal oocytes. 2007;134(2):241-252.
117. Li J, Balboula AZ, Aboelenain M, et al. Effect of autophagy induction and cathepsin B inhibition on developmental competence of poor quality bovine oocytes. 2019;
118. Song B-S, Kim J-S, Kim Y-H, et al. Induction of autophagy during in vitro maturation improves the nuclear and cytoplasmic maturation of porcine oocytes. 2014;26(7):974-981.
119. Bandyopadhyay A, Bandyopadhyay J, Chung J, Choi H-S, Kwon H-BJG, endocrinology c. Inhibition of S6 Kinase by Rapamycin Blocks Maturation ofRana dybowskiiOocytes. 1999;113(2):230-239.
120. Kim S, Cordeiro M, Serna V, et al. Rescue of platinum-damaged oocytes from programmed cell death through inactivation of the p53 family signaling network. 2013;20(8):987-997.
121. Gonfloni S, Di Tella L, Caldarola S, et al. Inhibition of the c-Abl–TAp63 pathway protects mouse oocytes from chemotherapy-induced death. 2009;15(10):1179-1185.
122. Woodruff TKJNm. Preserving fertility during cancer treatment. 2009;15(10):1124-1125.
123. Chun EK, Jee BC, Kim JY, Kim SH, Moon SYJRs. Effect of imatinib coadministration on in vitro oocyte acquisition and subsequent embryo development in cyclophosphamide-treated mice. 2014;21(7):906-914.
124. Salem W, Ho JR, Woo I, et al. Long-term imatinib diminishes ovarian reserve and impacts embryo quality. 2020;37(6):1459-1466.
125. Adhikari D, Risal S, Liu K, Shen YJPo. Pharmacological inhibition of mTORC1 prevents over-activation of the primordial follicle pool in response to elevated PI3K signaling. 2013;8(1):e53810.

126. Zhang X-m, Li L, Xu J-j, et al. Rapamycin preserves the follicle pool reserve and prolongs the ovarian lifespan of female rats via modulating mTOR activation and sirtuin expression. 2013;523(1):82-87.
127. Adhikari D, Flohr G, Gorre N, et al. Disruption of Tsc2 in oocytes leads to overactivation of the entire pool of primordial follicles. 2009;15(12):765-770.
128. Dou X, Sun Y, Li J, et al. Short-term rapamycin treatment increases ovarian lifespan in young and middle-aged female mice. 2017;16(4):825-836.
129. Zamah AM, Mauro MJ, Druker BJ, et al. Will imatinib compromise reproductive capacity? 2011;16(10):1422-1427.
130. Maiani E, Di Bartolomeo C, Klinger FG, et al. Reply to: Cisplatin-induced primordial follicle oocyte killing and loss of fertility are not prevented by imatinib. 2012;18(8):1172-1174.

7. APPENDICES

7.1. Ethical Approval

T.C. YEDİTEPE ÜNİVERSİTESİ
Hayvan Deneyleri Yerel Etik Kurulu (HADYEK)

ETİK KURUL KARARI

Protokol No	Toplantı Tarihi	Toplantı Sayısı	Karar No	Proje Yürütücüsü
2021-031	03.06.2021	2021/06	2021/06-5	Doç. Dr. Aylin Yaba Uçar

'Fare Oosit Maturasyonunda c-Abl Tirozin Kinaz ve Memeli Rapamisin Hedefi (mTOR) Düzenlenmesinin Belirlenmesi' isimli proje oy birliğiyle etik açıdan uygun görülmüştür.

Hayvan Türü / Irkı	Toplam Hayvan Sayısı	Hayvanın Cinsiyeti
Fare / BALB/c	18	Dişi

Görevi	Adı Soyadı	Katılım Durumu
Başkan	Prof. Dr. Bayram YILMAZ	
Başkan Vekili	Prof. Dr. Erdem YEŞİLADA	
Üye	Dr. Veteriner Hekim Engin SÜMER	
Üye	Prof. Dr. M. Ece GENÇ	
Üye	Prof. Dr. Rukset ATTAR	
Üye	Prof. Dr. Gamze TORUN KÖSE	
Üye	Doç. Dr. Ediz DENİZ	Katılmadı
Üye	Doç. Dr. Aylin YABA UÇAR	Katılmadı
Üye	Doç. Dr. Burcu GEMİCİ BAŞOL	
Üye	Hakan GÖKSEL	
Üye	Ahmet ŞENKARDEŞLER	

8. CURRICULUM VITAE

Personal Information

Name	Melek	**Surname**	OBAIDEEN
Place of birth		**Date of birth**	
Nationality		**TC Kimlik No**	
E-mail		**Phone**	

Education status

Degree	**Department**	**Name of Graduate Institution**	**Graduation date**
Licence	Bioengineering	Kırıkkale University, Faculty of Engineering	2018-2019
High school	Health high school	Health high school	2010-2011

Foreign Language	**Foreign Language Exam Score**
Turkish	TOMER 84
English	YDS 60